

# Nonlinear Viscoelasticity and Viscoplasticity Characteristics of Virgin and Modified Asphalt Binders

Hui Li, Ph.D.

1, School of Transportation, Southeast University, Nanjing, 211189, China.

2, Department of Civil and Environmental Engineering

The Hong Kong Polytechnic University

Hung Hom, Kowloon, Hong Kong

Email: [huili94@seu.edu.cn](mailto:huili94@seu.edu.cn)

Jian Ling

College of Civil Engineering and Architecture

Zhejiang University

866 Yuhangtang Road,

Hangzhou 310058, Zhejiang, China

Email: [22012303@zju.edu.cn](mailto:22012303@zju.edu.cn)

Zhen Leng, Ph.D.

Department of Civil and Environmental Engineering

The Hong Kong Polytechnic University

Hung Hom, Kowloon, Hong Kong

Email: [zhen.leng@polyu.edu.hk](mailto:zhen.leng@polyu.edu.hk)

Yuqing Zhang, Ph.D.

School of Transportation

Southeast University

Nanjing, 211189, China.

Email: [zhangyuqing@seu.edu.cn](mailto:zhangyuqing@seu.edu.cn)

Xue Luo, Ph.D.

College of Civil Engineering and Architecture

Zhejiang University

866 Yuhangtang Road,

Hangzhou 310058, Zhejiang, China

Phone: (86) 571-88206542

Email: [xueluo@zju.edu.cn](mailto:xueluo@zju.edu.cn)

41    **Abstract**

42    Many engineering materials have coupled nonlinear viscoelasticity and viscoplasticity, which are  
43    affected by complex thermo-mechanical loadings. This study aims to address the challenge of  
44    accurately separating the viscoplasticity and the nonlinear viscoelasticity and formulate the  
45    viscoplasticity by considering the effects of temperatures and loading levels. First, the nonlinear  
46    viscoelastic constitutive equation is adopted to accurately separate the viscoplasticity and the  
47    nonlinear viscoelasticity. Then, a kinetics-based viscoplastic model and a new viscoplastic activation  
48    energy indicator are proposed to consider the effects of the temperature and loading level on the  
49    viscoplasticity. As typical nonlinear viscoelastic viscoplastic materials commonly used in pavement  
50    engineering, asphalt binders are selected to demonstrate the principles in this study. It was found that  
51    the proportion of the viscoplastic strain is larger than the nonlinear viscoelastic strain for virgin  
52    asphalt binders (VB) and it increases with the temperature, while high-viscosity modified asphalt  
53    binders (HVB) and rubber asphalt binders (RB) are opposite. The logarithm of the viscoplastic strain  
54    rate is linearly increased with the reciprocal of the temperature, and the viscoplastic strain rates at  
55    different temperatures are correlated and can be predicted based on the established viscoplastic strain  
56    kinetics model. The viscoplastic activation energy indicator can characterize the viscoplastic  
57    deformation resistance for nonlinear viscoelastic viscoplastic materials, and the order of the  
58    viscoplastic deformation resistances of the three binders is:  $VB < HVB < RB$ , based on this indicator.

59

60    **Keywords:** viscoplasticity; nonlinear viscoelasticity; kinetics-based viscoplastic model; viscoplastic  
61    activation energy

62

63

64

65

66

67

68

## 69    **1 Introduction**

70    Many engineering materials have coupled nonlinear viscoelasticity and viscoplasticity, which are  
71    affected by complex thermo-mechanical loadings, and the viscoplasticity will affect the service  
72    performance of the structures where these materials are used. Hence, it is necessary to investigate  
73    and model the viscoplasticity by considering the influence of the temperature and loading level on  
74    engineering materials. A representative nonlinear viscoelastic viscoplastic material, asphalt binder,  
75    widely used in pavement engineering, is selected for investigation in this study. Permanent  
76    deformation in the asphalt layer is one of the main diseases of asphalt pavements, which is mainly  
77    caused by the viscoplasticity of asphalt materials at a high temperature and overloading. The  
78    permanent deformation, also known as rutting, of asphalt pavements, can shorten the service life of  
79    asphalt pavements, compromise ride quality, and more seriously, bring safety hazards. It should be  
80    pointed out that the mechanical properties of asphalt binders play an important role in the rutting  
81    performance of asphalt mixtures and pavements (D'Angelo 2009; Tabatabaee & Tabatabaee 2010;  
82    Laukkanen et al., 2015; Walubita et al., 2022; Singh & Kumar., 2022).

83        Many indicators have been developed to indicate the viscoplastic performance of asphalt  
84    binders, such as rutting factor  $G^*/\sin\delta$  ( $G^*$  is shear modulus,  $\delta$  is phase angle) (Kennedy et al.,1994),  
85    zero shear viscosity (Sybilski, D. 1996), low shear viscosity (Morea et al., 2011) and the viscous  
86    component of the creep stiffness (Bahia et al., 2001). These indicators have been successfully applied  
87    to different types of asphalt binders (Lu et al., 2023; Shirzad et al., 2023; Padhan et al., 2020; Leng et  
88    al., 2018a; 2018b). However, these indicators have a limitation that they were established by only  
89    considering the linear viscoelastic property of asphalt binders, while many asphalt binders may have  
90    an obvious nonlinear viscoelastic characteristic, and the impact of nonlinear viscoelasticity of asphalt  
91    binder cannot be negligible (Tsantilis et al. 2021; Delgadillo et al., 2012; Masad et al. 2009; Nivitha  
92    et al., 2018; Sun et al., 2020).

93        Non-recoverable creep compliance is an indicator which can characterize the viscoplastic  
94    deformation of asphalt binders (D'Angelo et al., 2009). It should be noted that the non-recoverable  
95    creep compliance indicator includes the influence of the nonlinear viscoelasticity of asphalt binders.  
96    The standard non-recoverable creep compliance indicator can be determined through the creep and

recovery test (AASHTO 2014), which consists of two stress levels (0.1 and 3.2kPa). Each stress level has 10 load-and-recovery cycles, and in each cycle, creep is applied for 1.0 second followed by 9.0 seconds rest period. The indicator can be determined by the strain at the end of the recovery phase, i.e., using this strain as the non-recoverable strain of the asphalt binders. However, the accumulation creep strains of the asphalt binder cannot be recovered in a short time, and Delgadillo et al., 2012 reported that the strain recovery rate is 98% for the modified asphalt binder after 1,000 s recovery when the test temperature is 46°C. In practice, the nonlinear viscoelastic strain of asphalt binders cannot be completely recovered in a finite time. Therefore, it is not feasible to obtain the precise non-recoverable creep compliance for all asphalt binders based on the test results of the creep and recovery tests.

Schapery proposed a nonlinear viscoelastic constitutive equation by irreversible thermodynamic descriptions of the state for nonlinear viscoelastic materials (Schapery 1966; 1969). The problem of the nonlinear viscoelasticity of asphalt binders cannot be completely recovered in a finite time in the creep and recovery phase can be solved according to Schapery's pioneering work. Some researchers employed Schapery's nonlinear viscoelastic constitutive equation to obtain the nonlinear viscoelastic and non-recoverable viscoplastic strain for asphalt binders. Masad et al. (2009) separated the recoverable (nonlinear viscoelastic) strain from the non-recoverable (viscoplastic) strain and determined the nonlinear viscoelastic parameters for the asphalt binders based on Schapery's nonlinear viscoelastic constitutive equation. Sadeq et al. (2016) analyzed the linear and nonlinear viscoelastic and viscoplastic strain of the asphalt binders with warm mix asphalt additives according to the research of Masad et al. (2009). Liu et al. (2021) analyzed the steady-state strain response under the stress level of 0.1 and 3.2 kPa by Schapery's nonlinear viscoelastic constitutive equation and analyzed the test results of the asphalt binders with improved accuracy. In these studies, the non-recoverable creep compliance of asphalt binders was redefined by the viscoplastic strain obtained from Schapery's nonlinear viscoelastic constitutive equation. These studies have great significance to accurately characterize the viscoplastic performance of asphalt binders, but the effect of temperature on the asphalt binders is not considered in these studies.

The mechanical behavior of nonlinear viscoelastic viscoplastic materials is closely related to

temperature and loading level. It will gradually soften as the temperature increases, and large amounts of energy is needed to drive viscoplastic deformation. On the contrary, when the materials become stiff with the reduction of the temperature, the energy required to produce viscoplastic deformation is reduced. Besides, the evolution rate of viscoplastic deformation is certainly affected by the temperature. The high loading level will also increase the viscoplastic deformation of the materials, while the low loading level is the opposite. Therefore, the temperatures and loading levels are very significant factors for viscoplasticity. To address this issue, the objective of this study is to investigate the viscoplasticity coupled with nonlinear viscoelasticity and propose a new evaluation indicator of the viscoplasticity that considers the effects of the temperatures and loading levels for the nonlinear viscoelastic viscoplastic materials, and asphalt binders (typical nonlinear viscoelastic viscoplastic materials) are selected to demonstrate the principles.

To achieve the objective of this study, the following research tasks were conducted. First, a nonlinear viscoelastic viscoplastic constitutive model is established, and a kinetics-based viscoplastic model and a new viscoplastic activation energy indicator for nonlinear viscoelastic viscoplastic materials were proposed. Then, three types of asphalt binders are selected to demonstrate the principles. Finally, analysis was conducted on the mechanical model parameters (Prony series coefficients and nonlinear viscoelastic parameters), the nonlinear viscoelasticity and viscoplasticity, the kinetics-based viscoplastic model and viscoplastic activation energy indicator.

## 2 Mechanical and kinetics modeling for nonlinear viscoelasticity and viscoplasticity

Boltzmann's superposition principle is widely used to describe the linear viscoelastic constitutive relationship of materials with a time-dependent response (Brinson & Brinson 2008), and a general three-dimensional linear viscoelastic constitutive model may be written as follows:

$$\varepsilon_{ij}^{ve} = D_{ijkl}(0)\sigma_{ij} + \int_0^t \Delta D_{ijkl}(t-\tau) \frac{\partial \sigma_{ij}}{\partial \tau} d\tau \quad (1)$$

where  $\varepsilon_{ij}^{ve}$  and  $\sigma_{ij}$  are linear viscoelastic strain tensor and stress tensor of the materials, respectively;  $D_{ijkl}(0)$  is instantaneous compliance tensor;  $\Delta D_{ijkl}$  is transient compliance

151 component tensor; and  $\tau$  is the arbitrary time between 0 and  $t$ .

152 Considering that some engineering materials show obvious nonlinear viscoelastic characteristics,  
 153 Schapery (1966, 1969) developed a nonlinear viscoelastic constitutive equation for the nonlinear  
 154 viscoelastic materials which show the nonlinear viscoelastic characteristics based on irreversible  
 155 thermodynamic descriptions of the state, and the three-dimensional nonlinear viscoelastic  
 156 constitutive equation can be expressed by:

$$157 \quad \varepsilon_{ij}^{nve} = g_0 D_{ijkl}(0) \sigma_{ij} + g_1 \int_{0^-}^t \Delta D_{ijkl}(\psi - \psi') \frac{\partial g_2 \sigma_{ij}}{\partial \tau} d\tau \quad (2)$$

158 where  $\varepsilon_{ij}^{nve}$  is nonlinear viscoelastic strain tensor of the materials;  $g_0$ ,  $g_1$  and  $g_2$  are nonlinear  
 159 viscoelastic parameters of the materials, which due to third and higher-order dependence of Gibb's  
 160 free energy on the applied stress;  $\psi$  and  $\psi'$  are reduced-time, which are defined by:

$$161 \quad \psi = \psi(t) = \int_{0^-}^t dt / a_\sigma(\sigma_{ij}) \quad (3)$$

$$162 \quad \psi' = \psi(\tau) = \int_{0^-}^\tau dt / a_\sigma(\sigma_{ij}) \quad (4)$$

163 in which  $a_\sigma$  is shift factor. In general, the shift factor results from similar higher-order effects of  
 164 entropy production and free energy.

165 It should be noted that the nonlinear viscoelastic constitutive equation for nonlinear viscoelastic  
 166 materials degrades to the linear viscoelastic constitutive equation when these nonlinear viscoelastic  
 167 parameters are equal to one, i.e.,  $g_0 = g_1 = g_2 = a_\sigma = 1$ . In this study, creep and recovery tests are  
 168 performed and two-step stress (loading step and unloading step) are contained. To more generally  
 169 model the nonlinear viscoelastic characteristics, general two-step stress tensor is selected to study the  
 170 nonlinear viscoelastic constitutive equation for nonlinear viscoelastic materials, and two-step stress  
 171 tensor can be expressed by:

$$172 \quad \sigma_{ij}(t) = \sigma_p H(t) I_{ij} - (\sigma_p - \sigma_q) H(t - t_p) I_{ij} \quad (5)$$

173 where  $\sigma_p$  and  $\sigma_q$  are magnitudes of two arbitrary constant stresses tensor  $\sigma_p I_{ij}$  and  $\sigma_q I_{ij}$ ,  
 174 respectively;  $I_{ij}$  is unit second order tensor;  $t_p$  represents the moment when the  $\sigma_p I_{ij}$  is

175 unloading;  $H(t)$  is Heaviside unit-step function, which can be defined as below:

$$176 \quad H(t-t_q) = \begin{cases} 0 & t \leq t_q \\ 1 & t > t_q \end{cases} \quad (6)$$

177 For two constant stress tensors, the nonlinear viscoelastic parameters are also constant at respective  
178 loading time. Substituting Eqs. (5) and (6) into the nonlinear viscoelastic constitutive equation (Eq.  
179 (2)), the strain response of the nonlinear viscoelastic materials can be expressed as below:

$$180 \quad \begin{aligned} \varepsilon_{ij}^{nve} = & g_0^p \sigma_p H(t) D_{ijkl}(0) I_{ij} + (g_0^q \sigma_q - g_0^p \sigma_p) H(t-t_p) D_{ijkl}(0) I_{ij} \\ & + g_1^p \int_{0^-}^t \Delta D_{ijkl}(\psi - \psi') \frac{d}{d\tau} \left( g_2^p \sigma_p H(\tau) I_{ij} + (g_2^q \sigma_q - g_2^p \sigma_p) H(\tau-t_p) I_{ij} \right) d\tau \end{aligned} \quad (7)$$

181 where  $g_0^p$ ,  $g_1^p$ ,  $g_2^p$  and  $a_\sigma^p$  are nonlinear viscoelastic parameters of  $\sigma_p I_{ij}$ ;  $g_0^q$ ,  $g_1^q$ ,  $g_2^q$  and  $a_\sigma^q$   
182 are nonlinear viscoelastic parameters of  $\sigma_q I_{ij}$ .

183 Eq. (7) can be divided into two parts, and the form of Eq. (7) can be written as follows:

$$184 \quad \begin{aligned} \varepsilon_{ij}^{nve} = & g_0^p \sigma_p H(t) D_{ijkl}(0) I_{ij} + (g_0^q \sigma_q - g_0^p \sigma_p) H(t-t_p) D_{ijkl}(0) I_{ij} \\ & + g_1^p \int_{0^-}^{t_p} \Delta D_{ijkl}(\psi - \psi') \left( g_2^p \sigma_p I_{ij} \frac{dH(\tau)}{d\tau} + (g_2^q \sigma_q - g_2^p \sigma_p) I_{ij} \frac{dH(\tau-t_p)}{d\tau} \right) d\tau \\ & + g_1^q \int_{t_p}^t \Delta D_{ijkl}(\psi - \psi') \left( g_2^p \sigma_p I_{ij} \frac{dH(\tau)}{d\tau} + (g_2^q \sigma_q - g_2^p \sigma_p) I_{ij} \frac{dH(\tau-t_p)}{d\tau} \right) d\tau \end{aligned} \quad (8)$$

185 where  $\frac{dH(\tau)}{d\tau} = \delta(\tau)$ ,  $\frac{dH(\tau-t_p)}{d\tau} = \delta(\tau-t_p)$ ; and  $\delta(\tau-t_p)$  is Dirac delta function, which has  
186 the following expression:

$$187 \quad \begin{cases} \delta(\tau-t_p) = 0 & t \neq t_p \\ \int_{-\infty}^{+\infty} \delta(\tau-t_p) d\tau = 1 \end{cases} \quad (9)$$

188 Ignoring the term whose value is zero, the expression can be simplified as follows:

$$189 \quad \begin{aligned} \varepsilon_{ij}^{nve} = & g_0^p \sigma_p H(t) D_{ijkl}(0) I_{ij} + (g_0^q \sigma_q - g_0^p \sigma_p) H(t-t_p) D_{ijkl}(0) I_{ij} \\ & + g_1^p \int_{0^-}^{t_p} \Delta D_{ijkl}(\psi - \psi') g_2^p \sigma_p I_{ij} \delta(\tau) d\tau + g_1^q \int_{t_p}^t \Delta D_{ijkl}(\psi - \psi') (g_2^q \sigma_q - g_2^p \sigma_p) I_{ij} \delta(\tau-t_p) d\tau \end{aligned} \quad (10)$$

190 When  $0 \leq t \leq t_p$ , only the constant stress tensor  $\sigma_p I_{ij}$  is applied for the materials. Eq. (10) can be

191 written as:

$$192 \quad \varepsilon_{ij}^{nve} = g_0^p \sigma_p H(t) D_{ijkl}(0) I_{ij} + g_1^p \int_{0^-}^{t_p} \Delta D_{ijkl} (\psi - \psi') g_2^p \sigma_p I_{ij} \delta(\tau) d\tau \quad (11)$$

193 It can be seen from Eq. (11) that the values of  $\delta(\tau)$  are zero except for  $\tau = 0$ . Therefore, the  
194 reduced time can be calculated by the following expressions:

$$195 \quad \psi = \psi(t) = \int_{0^-}^t dt / a_\sigma (\sigma_{ij} = \sigma_p I_{ij}) = \frac{t}{a_\sigma^p} \quad (12)$$

$$196 \quad \psi' = \psi(\tau) = \int_0^\tau dt / a_\sigma (\sigma_{ij} = \sigma_p I_{ij}) = \frac{\tau}{a_\sigma^p} = 0 \quad (13)$$

197 Substituting Eqs. (12) and (13) into Eq. (10), the following simplified expression of strain can be  
198 obtained:

$$199 \quad \varepsilon_{ij}^{nve} = \left[ g_0^p \sigma_p D_{ijkl}(0) I_{ij} + g_1^p g_2^p \Delta D_{ijkl} \left( \frac{t}{a_\sigma^p} \right) \sigma_p I_{ij} \right] H(t), \quad 0 \leq t \leq t_p \quad (14)$$

200 Similarly, when  $t > t_p$ , the constant stress tensor  $\sigma_q I_{ij}$  is applied to the materials, Eq. (10) can be  
201 rewritten as:

$$202 \quad \begin{aligned} \varepsilon_{ij}^{nve} = & g_0^q \sigma_q H(t - t_p) D_{ijkl}(0) I_{ij} + g_1^q \int_{0^-}^{t_p} \Delta D_{ijkl} (\psi - \psi') g_2^p \sigma_p I_{ij} \delta(\tau) d\tau \\ & + g_1^q \int_{t_p}^t \Delta D_{ijkl} (\psi - \psi') (g_2^q \sigma_q - g_2^p \sigma_p) I_{ij} \delta(\tau - t_p) d\tau \end{aligned} \quad (15)$$

203 Eq. (15) contains two integral terms: the first integral term is caused by the constant stress tensor  
204  $\sigma_p I_{ij}$  at  $t = 0$  and the second integral term is affected by the constant stress tensor  $\sigma_q I_{ij}$  at  $t = t_p$ .

205 Thus, the reduce-time of the first integral term can be determined as follows:

$$206 \quad \psi = \psi(t) = \int_{0^-}^{t_p} dt / a_\sigma (\sigma_{ij} = \sigma_p I_{ij}) + \int_{t_p}^t dt / a_\sigma (\sigma_{ij} = \sigma_q I_{ij}) = \frac{t_p}{a_\sigma^p} + \frac{t - t_p}{a_\sigma^q} \quad (16)$$

$$207 \quad \psi' = \psi(\tau) = \int_0^\tau dt / a_\sigma (\sigma_{ij} = \sigma_p I_{ij}) = \frac{\tau}{a_\sigma^p} = 0 \quad (17)$$

208 In addition, the reduce-time of the second integral term can be calculated by:



$$\psi = \psi(t) = \int_{t_p}^t dt / a_\sigma (\sigma_{ij} = \sigma_q I_{ij}) = \frac{t - t_p}{a_\sigma^q} \quad (18)$$

$$\psi' = \psi(\tau) = \int_{t_p}^\tau dt / a_\sigma (\sigma_{ij} = \sigma_q I_{ij}) = \frac{\tau - t_p}{a_\sigma^q} = 0 \quad (19)$$

Finally, substituting Eqs. (16), (17), (18), (19) into Eq. (15), the nonlinear viscoelastic strain of the nonlinear viscoelastic materials can be present by:

$$\varepsilon_{ij}^{nve} = g_0^q \sigma_q D_{ijkl}(0) I_{ij} + g_1^q g_2^p \sigma_p \Delta D_{ijkl} \left( \frac{t_p}{a_\sigma^p} + \frac{t - t_p}{a_\sigma^q} \right) I_{ij} + g_1^q (g_2^q \sigma_q - g_2^p \sigma_p) \Delta D_{ijkl} \left( \frac{t - t_p}{a_\sigma^q} \right) I_{ij}, \quad t > t_p \quad (20)$$

Therefore, when the general two-step stress tensor is applied to nonlinear viscoelastic materials, the nonlinear viscoelastic constitutive equation which is applicable to any two-step stress can be obtained.

For a special case of the general two-step stress, i.e.,  $\sigma_p = \sigma_0$  and  $\sigma_q = 0$ , substituting  $\sigma_p = \sigma_0$ ,

$\sigma_q = 0$  and  $g_0^q = g_1^q = g_2^q = a_\sigma^q = 1$  into Eq. (20), the following nonlinear viscoelastic constitutive

equation can be obtained:

$$\varepsilon_{ij}^{nve} = g_0^p \sigma_p D_{ijkl}(0) I_{ij} + g_1^p g_2^p \sigma_p \Delta D_{ijkl} \left( \frac{t}{a_\sigma^p} \right) I_{ij}, \quad 0 \leq t \leq t_p \quad (21)$$

$$\varepsilon_{ij}^{nve} = g_2^p \sigma_p \Delta D_{ijkl} \left( \frac{t_p}{a_\sigma^p} + t - t_p \right) I_{ij} - g_2^p \sigma_p \Delta D_{ijkl} (t - t_p) I_{ij}, \quad t > t_p \quad (22)$$

In addition, the viscoplastic strain will appear under the high stress for the nonlinear viscoelastic viscoplastic materials. The viscoplastic strain accumulates over time and is non-recoverable. Thus, a nonlinear viscoelastic constitutive equation that contains viscoplasticity can be obtained by adding the viscoplastic strain into Eqs. (21) and (22), which can be expressed by the following equations:

$$\varepsilon_{ij} = \varepsilon_{ij}^{nve} + \varepsilon_{ij}^{vp}(t) = g_0^p \sigma_p D_{ijkl}(0) I_{ij} + g_1^p g_2^p \sigma_p \Delta D_{ijkl} \left( \frac{t}{a_\sigma^p} \right) I_{ij} + \varepsilon_{ij}^{vp}(t), \quad 0 \leq t \leq t_p \quad (23)$$

$$\varepsilon_{ij} = \varepsilon_{ij}^{nve} + \varepsilon_{ij}^{vp}(t_p) = g_2^p \sigma_0 \Delta D_{ijkl} \left( \frac{t_p}{a_\sigma^p} + t - t_p \right) I_{ij} - g_2^p \sigma_0 \Delta D_{ijkl} (t - t_p) I_{ij} + \varepsilon_{ij}^{vp}(t_p), \quad t > t_p \quad (24)$$

where  $\varepsilon_{ij}$  is total strain tensor of the materials; and  $\varepsilon_{ij}^{vp}(t)$ ,  $\varepsilon_{ij}^{vp}(t_p)$  are the viscoplastic strain tensor of the materials at loading time  $t$  and  $t_p$ .

229 The next step is to simulate the viscoplastic deformation process of the nonlinear viscoelastic  
 230 viscoplastic materials. In this study, the viscoplastic strain of the materials is modeled by the  
 231 Perzyna-type viscoplastic model (Perzyna, 1966):

$$232 \quad \dot{\epsilon}_{ij}^{vp} = \Gamma \langle \Phi(f) \rangle^N \frac{\partial g}{\partial \sigma_{ij}} \quad (25)$$

233 where  $\dot{\epsilon}_{ij}^{vp}$  is the viscoplastic strain rate;  $\Gamma$  is the viscosity-related parameter;  $N$  is viscoplastic  
 234 rate-dependent exponent;  $f$  is viscoplastic yield surface function;  $g$  is viscoplastic plastic potential  
 235 function; The McCauley brackets in Eq. (25) imply that:

$$236 \quad \langle \Phi(f) \rangle = \text{if} [\Phi(f) \leq 0, 0, f / 1Pa] \quad (26)$$

237 However, only loading time and stress level are considered in Perzyna-type viscoplastic model.  
 238 Temperature, one of the most important factors affecting viscoplastic strain, is not considered in this  
 239 model. To consider the effect of the temperature on the viscoplasticity, a kinetics-based model will be  
 240 established to characterize the viscoplasticity for the nonlinear viscoelastic viscoplastic materials. In  
 241 kinetics theory, a rate constant is used to measure the time required for any physical or chemical  
 242 process to reach an equilibrium state. The minimum energy that promotes the development of a  
 243 certain physical or chemical process of the system is called the activation energy of the process,  
 244 which has different activation energy for different materials and different physical or chemical  
 245 processes. The activation energy of a certain physical or chemical process is only related to the  
 246 material. The Arrhenius equation is widely used to establish the relationship between rate constant  
 247 and activation energy for a certain physical or chemical process, which can be expressed as follows  
 248 (Bamford and Tipper, 1969):

$$249 \quad k = A_0 e^{-\frac{E_a}{RT}} \quad (27)$$

250 where  $k$  is the rate constant of a certain physical or chemical process,  $A_0$  is the pre-exponential  
 251 factor of the process;  $E_a$  is the activation energy of the process;  $R$  is the ideal gas constant; and  $T$  is  
 252 the absolute temperature of the process.

253 Kinetics theory has been used to characterize the fatigue damage, heal process of the asphalt  
 254 materials (Luo et al., 2020; Li et al., 2021). For example, Li et al. (2021) established a relationship

between fatigue cracking growth rate and temperature for asphalt binders based on the kinetics theory. Furthermore, the kinetics theory has also been used to correlate the modulus change rate with the temperature, and an aging prediction model has been established to characterize the aging process of the in-service asphalt pavement (Luo et al., 2015; 2017; 2018). In this study, the viscoplastic deformation process of the nonlinear viscoelastic viscoplastic materials is temperature- and stress-dependent, and the Arrhenius equation in kinetics theory is employed to introduce the temperature effect for the Perzyna-type viscoplastic model, thus Eq. (27) can be modified as:

$$\dot{\varepsilon}_{ij}^{vpT} = A_{vp} e^{-\frac{E_{avp}}{RT}} = \Gamma_0 \langle \Phi(f) \rangle^N \frac{\partial g}{\partial \sigma_{ij}} e^{-\frac{E_{avp}}{RT}} \quad (28)$$

where  $\dot{\varepsilon}_{ij}^{vpT}$  is the viscoplastic strain rate considering the effects of temperatures and stress;  $A_{vp}$  is the pre-exponential factor, which equals to the stress-dependent viscoplastic strain rate  $\Gamma_0 \langle \Phi(f) \rangle^N \frac{\partial g}{\partial \sigma_{ij}}$  at a reference temperature; and  $E_{avp}$  is the viscoplastic activation energy of the nonlinear viscoelastic viscoplastic materials.

Taking the logarithm of both sides of Eq. (28) yields:

$$\ln \dot{\varepsilon}_{ij}^{vpT} = \ln \left( \Gamma_0 \langle \Phi(f) \rangle^N \frac{\partial g}{\partial \sigma_{ij}} \right) - \frac{E_{avp}}{RT} \quad (29)$$

Finally, a kinetics-based viscoplastic model and a viscoplastic activation energy indicator for characterizing the viscoplasticity for the nonlinear viscoelastic viscoplastic materials can be accurately determined based on Eqs. (23), (24), (25), (28) and (29) by considering the influence of the temperature and loading level. According to Eq. (29), the greater the viscoplastic activation energy, the smaller the viscoplastic strain rate, i.e., the greater the energy required for producing the same viscoplastic strain rate. Therefore, this indicator can be used to evaluate the viscoplastic deformation resistance of the nonlinear viscoelastic viscoplastic materials.

### 3 Materials and test methods

#### 3.1 Materials

To validate the feasibility of the theoretical process above and the applicability of the new indicator for nonlinear viscoelastic viscoplastic materials, asphalt binders (typical nonlinear viscoelastic viscoplastic materials) were taken as examples of analysis. Three types of asphalt binders supplied by Hebei Transportation Investment Group Corporation in China were selected, including a virgin asphalt binder, a high-viscosity modified asphalt binder and a rubber asphalt binder, which were denoted as VB, HVB and RB, respectively. VB does not have any additives, HVB contains styrene–butadiene–styrene and other polymer additives, and RB has 30% of crumb rubber. The basic properties (penetration, softening point and ductility) of these binders were obtained in accordance with the Chinese specification, as listed in Table 1.

**Table 1.** Basic properties of asphalt binders

Properties	Unit	Virgin asphalt binder	High-viscosity modified asphalt binder	Rubber asphalt binder
Penetration at 25°C	0.1mm	25	75	50
Softening point	°C	71.7	91.0	87.8
Ductility (5 °C)	cm	>50	>20	>10

#### 3.2 Sample preparation

In this study, the Discovery Hybrid Rheometer (DHR) from TA Instruments was adopted to perform laboratory tests for three types of asphalt binders. 25 mm diameter parallel plates and a 1 mm gap were used. The main steps for preparing the asphalt binder samples include: (1) heat the asphalt binders by putting them into the oven; (2) pour the hot flow-state asphalt binders into the silicon rubber mould, and cool the asphalt binder sample to room temperature for some time; (3) take out the asphalt binder sample by flexing the silicon rubber mould; (4) adhere the asphalt binder sample to the lower parallel plate and press the top surface of the sample gently; (5) turn off the environmental chamber of the instrument and raise the temperature to soften the asphalt binder sample; (6) lower the upper parallel plate to the trim gap and then lock the rotating lever of the instrument; (7) trim the

needless asphalt binder by using the heated trim tool and lower the upper parallel plate to the target gap; and (8) accurately control the temperature of asphalt binder samples by liquid nitrogen and environmental chamber before starting the laboratory tests. Thus, the preparation of the asphalt binder sample was completed.

### **3.3 Test methods**

To investigate the viscoplasticity of the asphalt binder by accurately separating it from nonlinear viscoelasticity and propose a new evaluation indicator of the viscoplasticity that considers the influence of temperature, creep and recovery tests under a low-stress level and a high-stress level were performed on three types of asphalt binders (VB, HVB and RB).

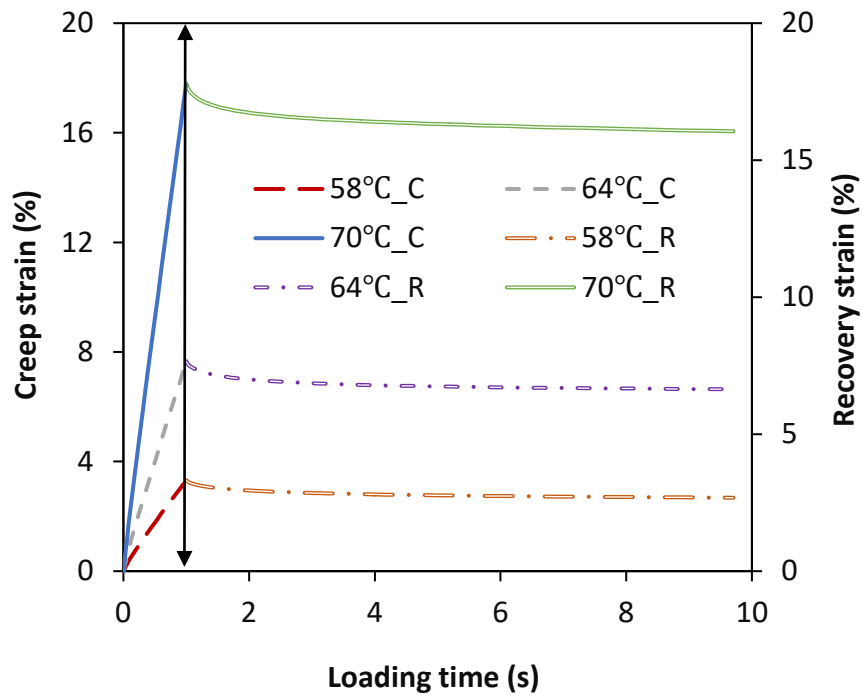
#### **3.3.1 Creep and recovery test under a low-stress level**

Some studies indicated that the linear viscoelastic information of the asphalt binders can be determined by the recovery strain at the creep stress of 0.1 kPa (Shirodkar, et al., 2012; Liu et al., 2021). The linear viscoelastic mechanical properties of asphalt binders were needed to determine the nonlinear viscoelastic parameters. Hence, the creep stress level of the creep and recovery test under a low-stress level was selected as 0.1kPa in this study, and the selected testing temperatures were 58°C, 64°C and 70°C for three types of asphalt binders (VB, HVB and RB). Taking the test results of VB as an example, Figure 1a shows the typical creep and recovery test results of the VB at 0.1kPa and three temperatures. In the legend, “\_C” stands for creep strain and “\_R” stands for recovery strain of the asphalt binders. It can be seen from Figure 1a that the loading time is 1s and the creep strain increases with the loading time during the creep phase, and the recovery time is 9s and the recovery strain decreases with the recovery time during the recovery phase. Besides, the creep strain and recovery strain increase with the increase of the temperature.

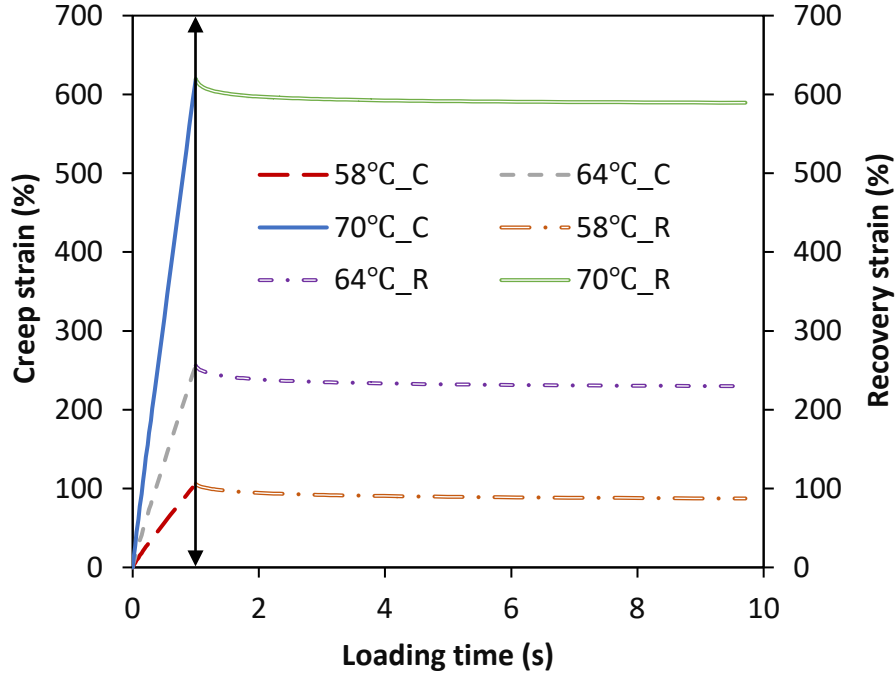
#### **3.3.2 Creep and recovery test under a high-stress level**

To investigate the nonlinear viscoelasticity and viscoplasticity of asphalt binders, the creep and recovery tests under a high-stress level were performed. The selected high-stress level was 3.2kPa.

327 To make sure the mechanical properties of the asphalt binder determined under the low-stress level  
 328 were applied to those under the high-stress level, the same testing temperatures (i.e., 58°C, 64°C and  
 329 70°C) were applied to the tests under the high-stress level. Similarly, taking the test results of VB as  
 330 an example, Figure 1b plots the typical creep and recovery test results of the VB at 3.2kPa and  
 331 different temperatures. The relationship trends of creep strain and recovery strain are the same as  
 332 Figure 1a, but the high-stress level can increase energy dissipation of the asphalt binders and induce  
 333 larger strain.



(a)



(b)

**Figure 1.** Typical creep and recovery test results of the VB at: (a) 0.1kPa; (b) 3.2kPa

## 4 Results and discussion

### 4.1 Mechanical model parameters

According to Eqs. (23) and (24), the total strain consists of nonlinear viscoelastic and viscoplastic strain. Before separating the viscoplastic strain and the nonlinear viscoelastic strain for three types of asphalt binders in this study, mechanical model parameters need to be first determined. There are two aspects: (1) determine the creep compliance based on the test results of the recovery test under the low-stress level (0.1kPa); and (2) obtain the nonlinear viscoelastic parameters according to the test results of the creep and recovery test under the high-stress level (3.2kPa).

#### 4.1.1 Determination of the creep compliances

When the one-dimensional constant stress is applied to the asphalt binder under linear viscoelastic condition, the creep compliance of the binder can be calculated by:

$$D(t) = \frac{\varepsilon(t)}{\sigma_p} \quad (30)$$

The Prony series model is widely used to analyze the creep compliance of asphalt materials (Luo, et al., 2020; Zhang, et al., 2016). In this study, the creep compliances of three types of asphalt binders are also modeled by the Prony series model:

$$D(t) = D_0 + \Delta D = D_0 + \sum_{i=1}^M D_i (1 - \exp(-t / \lambda_i)) \quad (31)$$

where  $\Delta D = D(t) - D_0$  represents the transient compliance;  $D_i$  is components of the creep compliance;  $\lambda_i$  is components of the retardation time;  $M$  is the total number of the Maxwell elements.

Furthermore, some studies show that the linear viscoelastic properties of the asphalt binder can be determined by the recovery strain under the creep stress of 0.1 kPa (Shirodkar, et al., 2012; Liu et al. 2021). Under the linear viscoelastic condition, the nonlinear viscoelastic parameters  $g_0^q$ ,  $g_1^q$ ,  $g_2^q$ ,  $a_\sigma^q$  are equal to one. Therefore, the recoverable linear viscoelastic strain in the recovery phase of the asphalt binder can be calculated based on Eqs. (23) and (24), and it can be expressed as:

$$\Delta \varepsilon_{ve} = [\Delta D(t_p) - \Delta D(t) + \Delta D(t - t_p)] \sigma_p \quad (32)$$

where  $\Delta \varepsilon_{ve}$  is the recoverable viscoelastic strain in the recovery phase of the asphalt binder.

According to the test results of the creep and recovery test, it can be found that the initial components of the creep compliance  $D_0$  are zero for three types of asphalt binders. Then, the other Prony series coefficients  $D_i$  and  $\lambda_i$  can be determined by Eq. (32) and the test results in the recovery phase of the asphalt binder based on the “Solve” tool in Excel. Taking the VB as an example, Figure 2 shows the test results and model values of the recoverable viscoelastic strain of VB at three temperatures (58°C, 64°C and 70°C). It can be seen that the model values can match the test data well at three temperatures for the VB, and the same findings apply to HVB and RB. It indicates that the Prony series can be used to model the creep compliance of the asphalt binders. The Prony series coefficients of the creep compliance of VB, HVB and RB at 64°C are shown in Table 2.



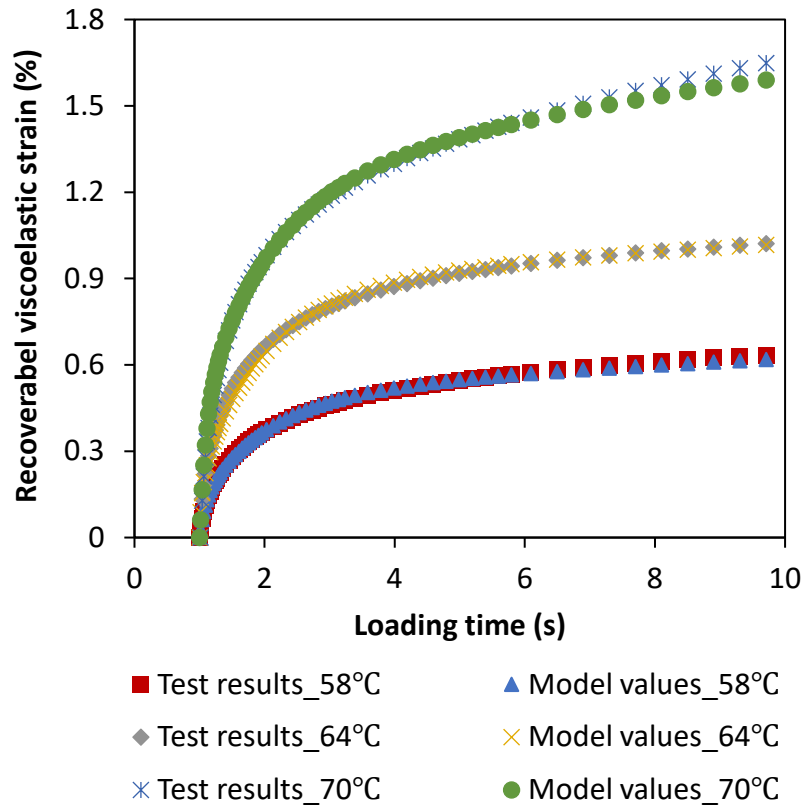


**Figure 2.** Test results and model values of the recoverable viscoelastic strain of VB at three temperatures (58°C, 64°C and 70°C)

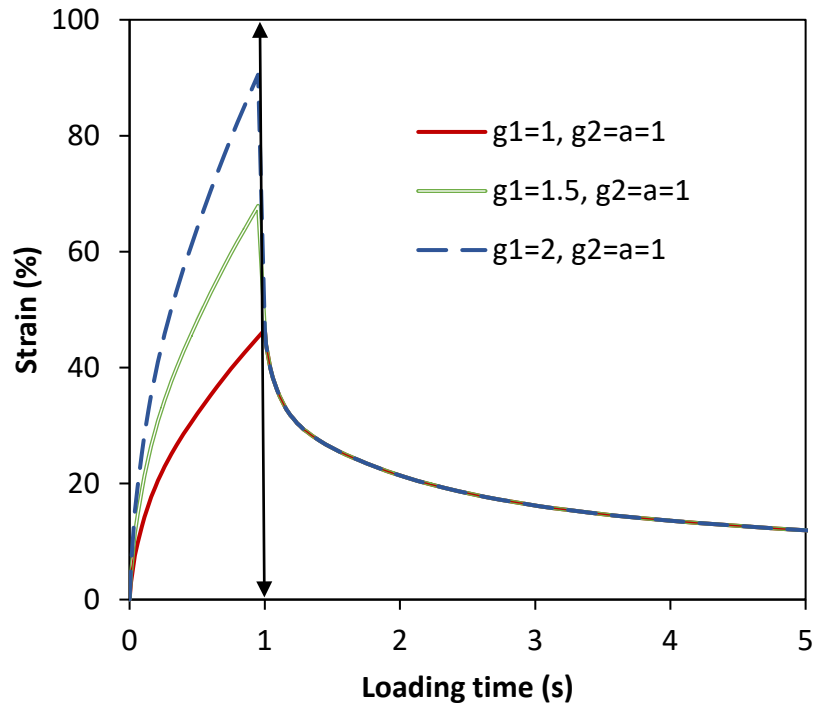
**Table 2.** Prony series coefficients of creep compliance of asphalt binders at 64°C

Materials		VB	HVB	RB
Components of creep compliance (1/kPa)	D <sub>1</sub>	0.27022	0.31474	0.40391
	D <sub>2</sub>	0.32163	2.19249	0.89889
	D <sub>3</sub>	0.09651	0.53762	0.14015
	D <sub>4</sub>	0.01373	0.21691	0.05142
	D <sub>5</sub>	0.00899	0.03895	0.01474
Components of retardation time (s)	λ <sub>1</sub>	100	100	100
	λ <sub>2</sub>	10	10	10
	λ <sub>3</sub>	1	1	1
	λ <sub>4</sub>	0.1	0.1	0.1
	λ <sub>5</sub>	0.01	0.01	0.01

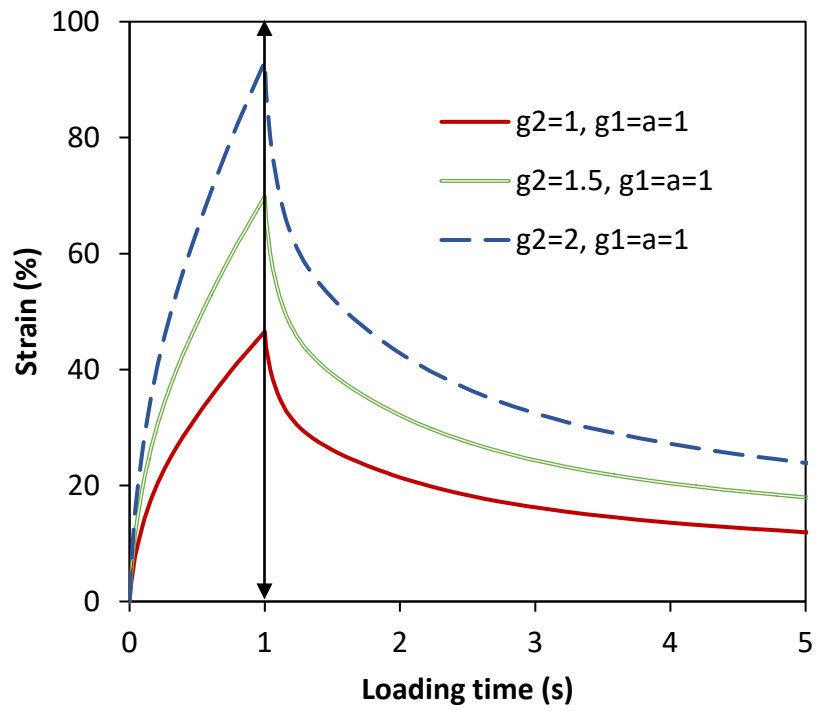
#### 4.1.2 Determination of the nonlinear viscoelastic parameters

To have a better understanding of the effects of the nonlinear viscoelastic parameters, the curves of

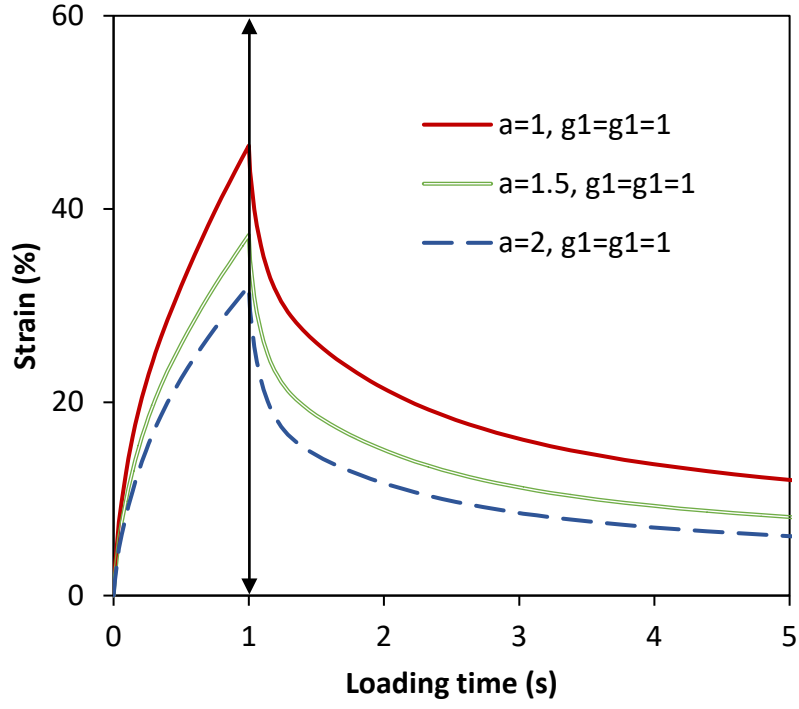
384 the strain vs loading time are plotted with some different values of nonlinear viscoelastic parameters.  
 385 Figure 3 presents the effects of different nonlinear parameters on the creep and recovery strain  
 386 response. Figure 3a shows the strain responses with different nonlinear viscoelastic parameters,  $g_1$ . It  
 387 shows that  $g_1$  influences the creep strain response, and the creep strain increases with the increase of  
 388  $g_1$ . However, the recovery strain responses keep unchanged with the increase of  $g_1$ . Figure 3b  
 389 presents the strain responses with different nonlinear viscoelastic parameters,  $g_2$ . It can be seen that  
 390 the creep and recovery strain responses increase with the increase of  $g_2$ . Figure 3c illustrates the  
 391 strain responses with different nonlinear viscoelastic parameters,  $a_\sigma$ . The creep strain and recovery  
 392 strain responses are both affected by  $a_\sigma$ , and decrease with the increase of  $a_\sigma$ . Besides, to more  
 393 clearly show the effect of the nonlinear viscoelastic parameters on the strain responses, Figure 3d  
 394 presents the change percentage of the strain responses when the nonlinear viscoelastic parameter is  
 395 1.5 ( $g_1 = g_2 = a_\sigma = 1.5$ ). The following conclusions can be obtained from Figure 3d: (1) the nonlinear  
 396 viscoelastic parameter  $g_1$  only affects the creep strain response of the materials, while the nonlinear  
 397 viscoelastic parameter  $g_2$  and  $a_\sigma$  both influence the creep and recovery strain response of the  
 398 materials; (2) the nonlinear viscoelastic parameter  $g_1$  and  $g_2$  have the same influence to the creep  
 399 strain response, and the effect values keep unchanged with the loading time; (3) the nonlinear  
 400 viscoelastic parameter  $a_\sigma$  decreases the creep and recovery strain responses, and the change  
 401 percentage of the strain first increases, and then decreases with the loading time in the creep phase,  
 402 and continuously decreases with the loading time in the recovery phase; and (4) the effect of  
 403 nonlinear viscoelastic parameter  $g_1$  and  $g_2$  on the strain response is more significant than that of the  
 404 nonlinear viscoelastic parameter  $a_\sigma$ .



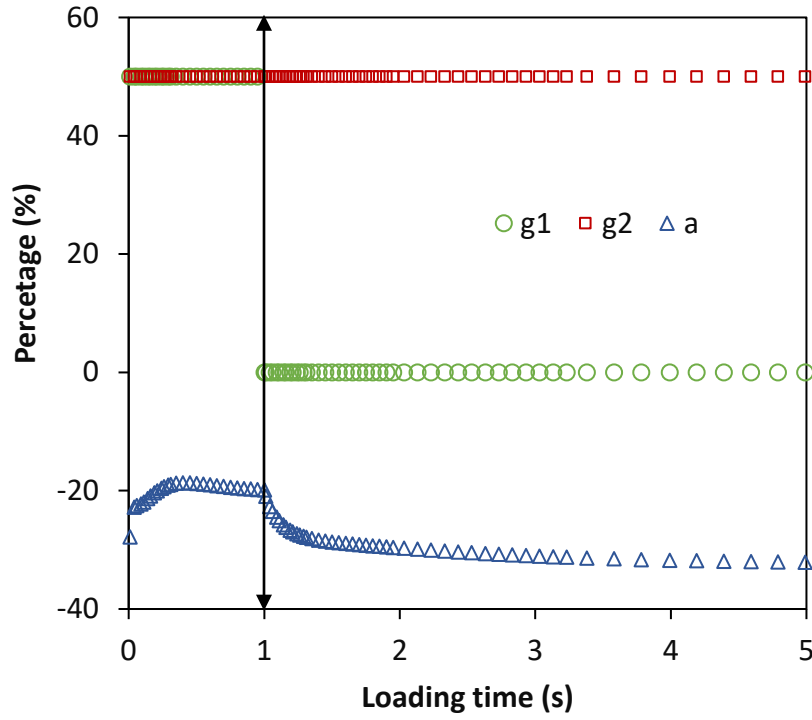
(a)



(b)



(c)



(d)

**Figure 3.** Strain responses at different nonlinear viscoelastic parameters and change percentage of the strain responses when  $g1 = g2 = a_\sigma = 1.5$ : (a) at different nonlinear viscoelastic parameters  $g1$ ; (b)

at different nonlinear viscoelastic parameters  $g_2$ ; (c) at different nonlinear viscoelastic parameters

$a_\sigma$ ; (d) change percentage of the strain response when  $g_1 = g_2 = a_\sigma = 1.5$

Hence, the nonlinear viscoelasticity of the materials is affected by these three nonlinear viscoelastic parameters together. In this study, the creep and recovery test under the high-stress level of 3.2kPa are performed on the asphalt binders, and the nonlinear viscoelastic characteristics are displayed. As introduced above, Eqs. (23) and (24) can be used to analyze the test results of the creep and recovery test for asphalt binders. It is noted that the expressions of strains are different when  $0 \leq t \leq t_p$  and  $t > t_p$ . When  $0 \leq t \leq t_p$ , the asphalt binder is in a creep phase. Thus, the strain at  $t = t_p^-$  can be determined as:

$$\varepsilon(t_p^-) = g_1^p g_2^p \Delta D\left(\frac{t_p^-}{a_\sigma^p}\right) + \varepsilon^{vp}(t_p^-, \sigma_0) \quad (33)$$

According to Eq. (33), the nonlinear viscoelastic strain can be obtained as:

$$\varepsilon(t_p^-) - \varepsilon^{vp}(t_p^-, \sigma_0) = g_1^p g_2^p \sigma_0 \Delta D\left(\frac{t_p^-}{a_\sigma^p}\right) \quad (34)$$

When  $t = t_p^+$ , the constant stress  $\sigma_0$  is removed, the nonlinear viscoelastic strain will gradually recover with the increase of recovery time. In addition, the viscoplastic strain is non-recoverable in the recovery phase, thus the strain at  $t = t_p^+$  can be calculated by:

$$\varepsilon(t_p^+) = g_2^p \sigma_0 \Delta D\left(\frac{t_p}{a_\sigma^p} + t_p^+ - t_p\right) - g_2^p \sigma_0 \Delta D(t_p^+ - t_p) + \varepsilon^{vp}(t_p^+, 0) \quad (35)$$

The viscoplastic strain is the same at  $t = t_p^-$  and  $t = t_p^+$ , that is  $\varepsilon^{vp}(t_p^-, \sigma_0) = \varepsilon^{vp}(t_p^+, 0)$ , and combining Eqs. (33) and (35), the following equation can be obtained:

$$\varepsilon(t_p^-) - \varepsilon(t_p^+) = g_2^p \sigma_0 \left[ g_1^p \Delta D\left(\frac{t_p^-}{a_\sigma^p}\right) - \Delta D\left(\frac{t_p}{a_\sigma^p} + t_p^+ - t_p\right) \right] + \sigma_0 \Delta D(t_p^+ - t_p) = g_2^p \sigma_0 \Delta D\left(\frac{t_p}{a_\sigma^p}\right) (g_1^p - 1) \quad (36)$$

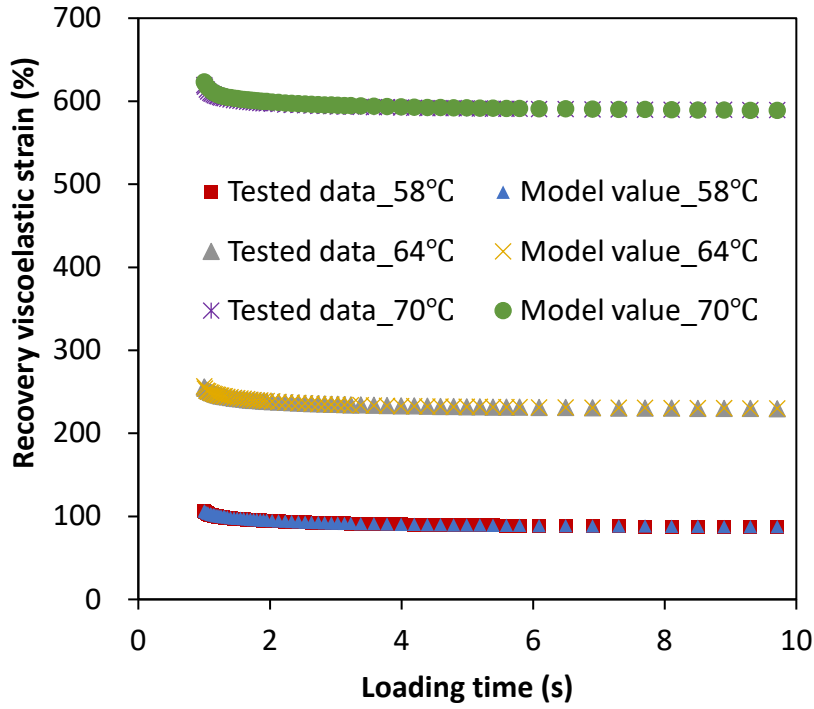
For the asphalt binders, the creep strain at  $t_p^-$  and the recovery strain at  $t_p^+$  are the same, i.e.,

$\varepsilon(t_p^-) = \varepsilon(t_p^+)$ . Thus, solving for  $g_1^p$  based on Eq. (36), i.e.,  $g_1^p = 1$ . This is an important conclusion

437 that the nonlinear parameter  $g_1^p$  of asphalt binders is always equal to one. Hence, the nonlinear  
 438 parameters  $g_0^p$  and  $g_1^p$  in nonlinear viscoelastic constitutive equation will not affect the nonlinear  
 439 viscoelastic behavior of the asphalt binders. Next, other nonlinear parameters  $g_2^p$  and  $a_\sigma^p$  for the  
 440 asphalt binders can be determined. Combining Eq. (24) in the recovery phase and Eq. (33) in the  
 441 creep phase of the asphalt binders, the expression of the nonlinear viscoelastic strain during the  
 442 recovery phase can be formulated as:

$$443 \quad \varepsilon(t) - \varepsilon(t_p^-) = g_2^p \sigma_0 \Delta D \left( \frac{t_p}{a_\sigma^p} + t - t_p \right) - g_2^p \sigma_0 \Delta D(t - t_p) - g_1^p g_2^p \Delta D \left( \frac{t_p}{a_\sigma^p} \right) \quad (37)$$

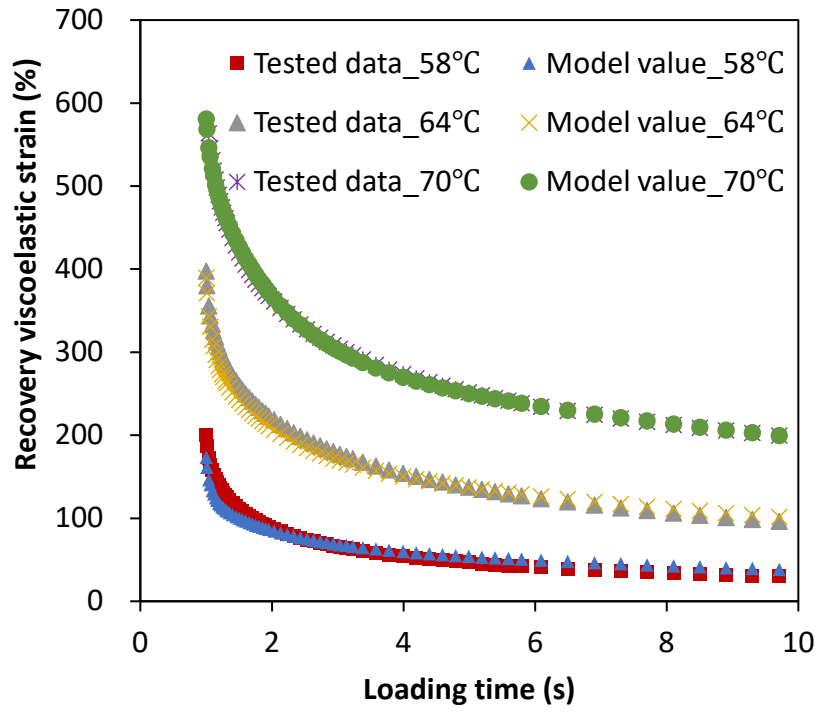
444 Solving the nonlinear parameters  $g_2^p$  and  $a_\sigma^p$  in Eq. (37) by fitting the test data in the recovery  
 445 phase of the asphalt binders. Figure 4 shows the test data and model values in the recovery phase  
 446 under the stress level of 3.2kPa at three temperatures (58°C, 64°C and 70°C) of VB, HVB and RB. It  
 447 can be seen from Figure 4 that the test data can match the model value calculated by Eq. (37) for all  
 448 binders at the three temperatures. Table 3 presents nonlinear viscoelastic parameters at the three  
 449 temperatures of the three types of asphalt binders.



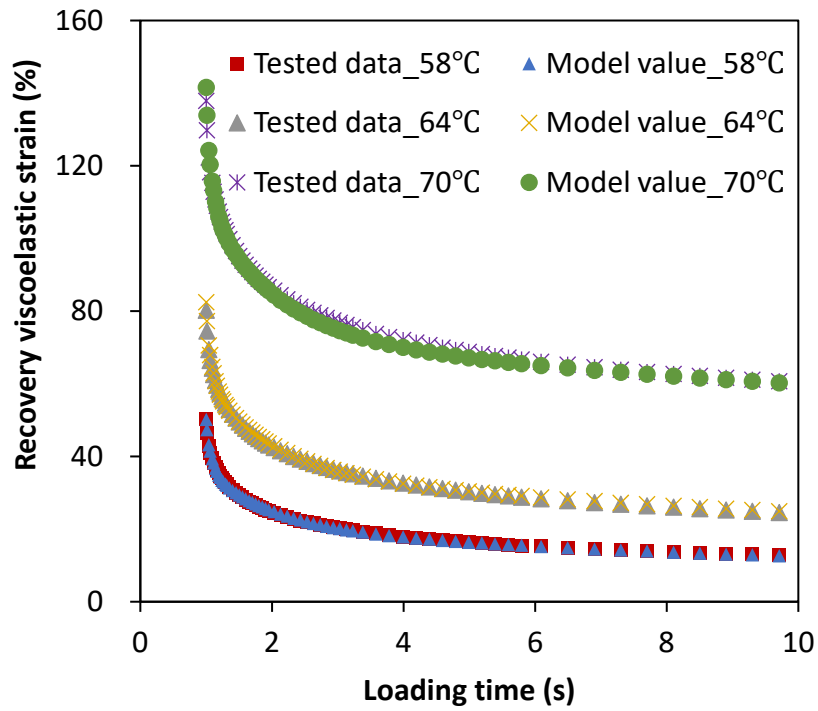
450

451

(a)



(b)



(c)

**Figure 4.** Test data and model values in the recovery phase under the stress level of 3.2kPa at three temperatures (58°C, 64°C and 70°C) of three types of asphalt binders (VB, HVB and RB): (a) VB; (b) HVB; (c) RB

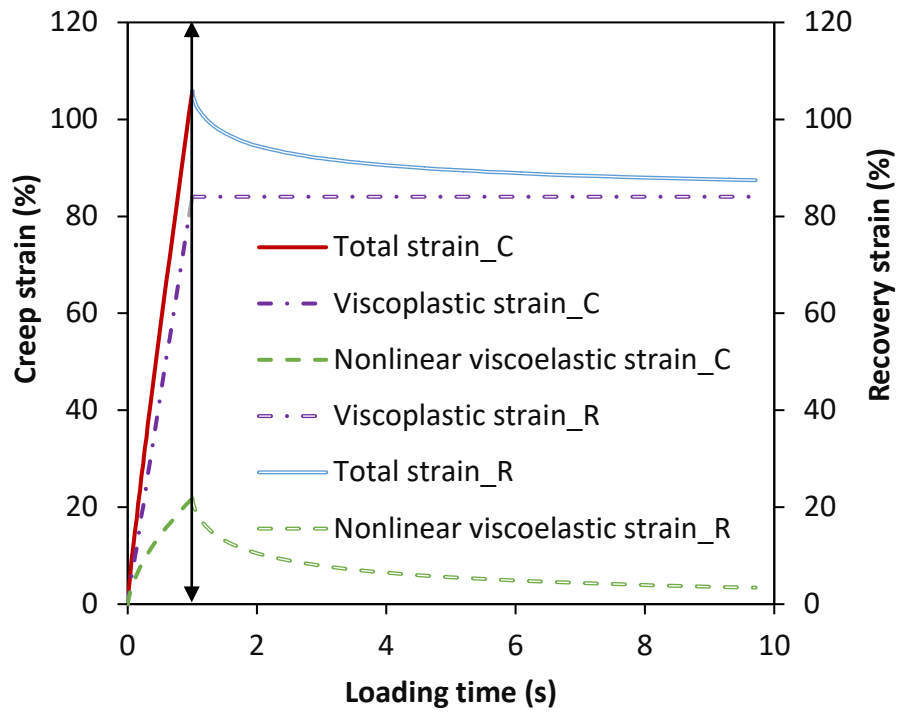
**Table 3.** Nonlinear viscoelastic parameters at three temperatures of three types of asphalt binders

Materials	VB			HVB			RB		
Parameters	$g_1^p$	$g_2^p$	$a_\sigma^p$	$g_1^p$	$g_2^p$	$a_\sigma^p$	$g_1^p$	$g_2^p$	$a_\sigma^p$
58°C	1	1.023	1.115	1	1.025	1.202	1	1.070	1.241
64°C	1	1.140	1.850	1	1.177	1.196	1	1.081	1.537
70°C	1	1.059	2.338	1	0.678	0.412	1	1.087	1.503

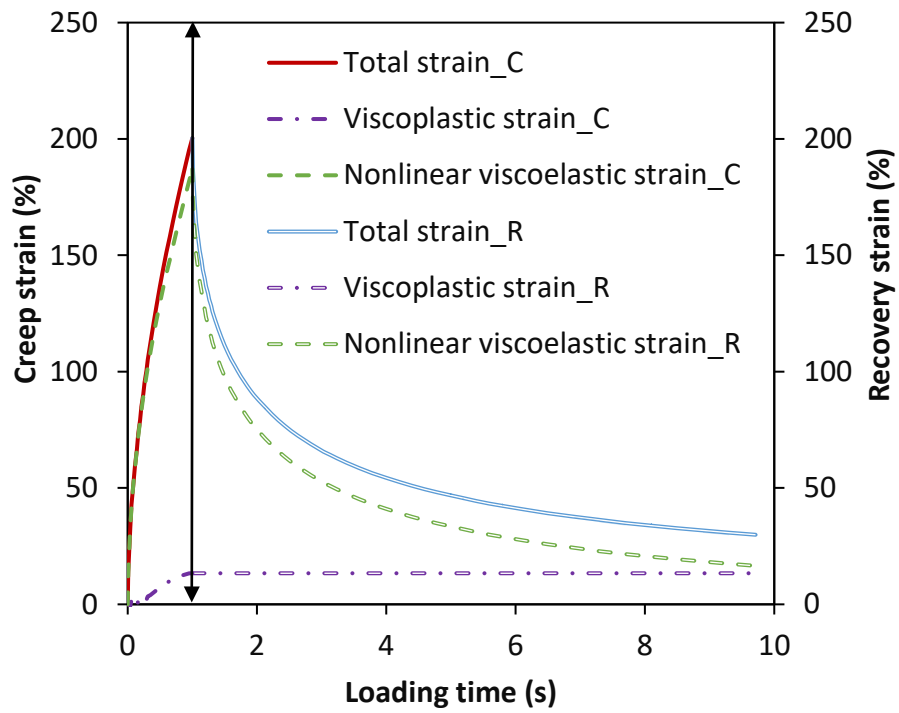
## 4.2 Nonlinear viscoelasticity and viscoplasticity

When the mechanical model parameters are determined, the nonlinear viscoelastic strain and viscoplastic strain can be separated based on the test results. Specifically, by substituting the mechanical model parameters into Eq. (21), the nonlinear viscoelastic strain of the asphalt binder can be determined. Then, combining the nonlinear viscoelastic parameters and Eq. (23), the viscoplastic strain can be accurately separated. Taking the analysis results of 58°C as an example, Figure 5 presents the nonlinear viscoelastic strain, viscoplastic strain and total strain in the creep and recovery phase of VB, HVB and RB at 58°C. In the legend, “\_C” stands for the strain response in the creep phase, and “\_R” stands for the strain response in the recovery phase. For example, “Total strain\_C” refers to the total creep strain and “Total strain\_R” refers to the total recovery strain of the asphalt binders. It can be seen from Figure 5 that the total creep strain consists of nonlinear viscoelastic strain and viscoplastic strain in the creep and recovery phase. Hence, the nonlinear viscoelastic strain and viscoplastic strain can be clearly separated based on the analysis in this study.

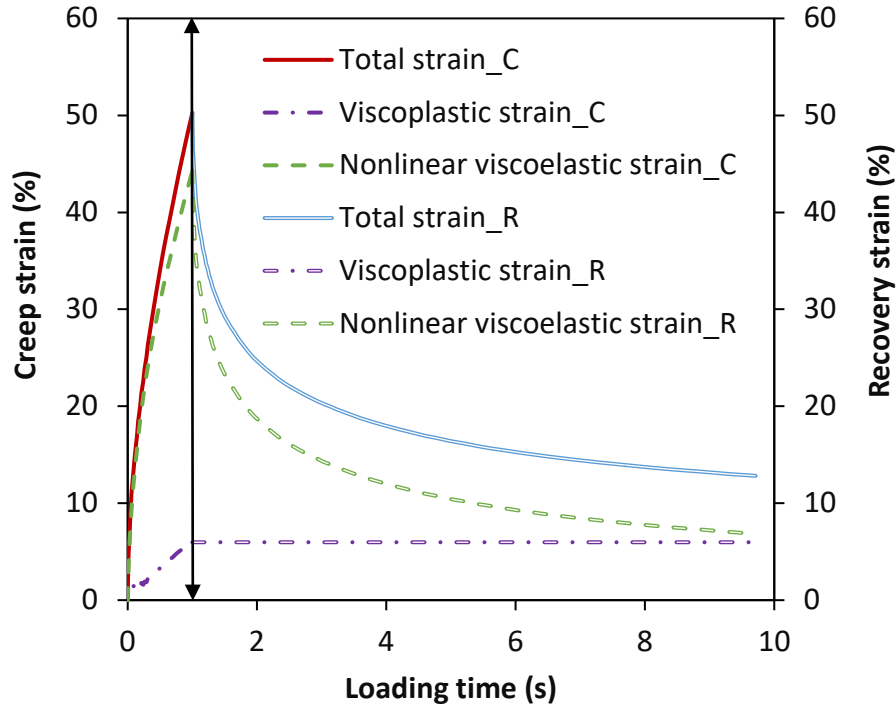




(a)



(b)

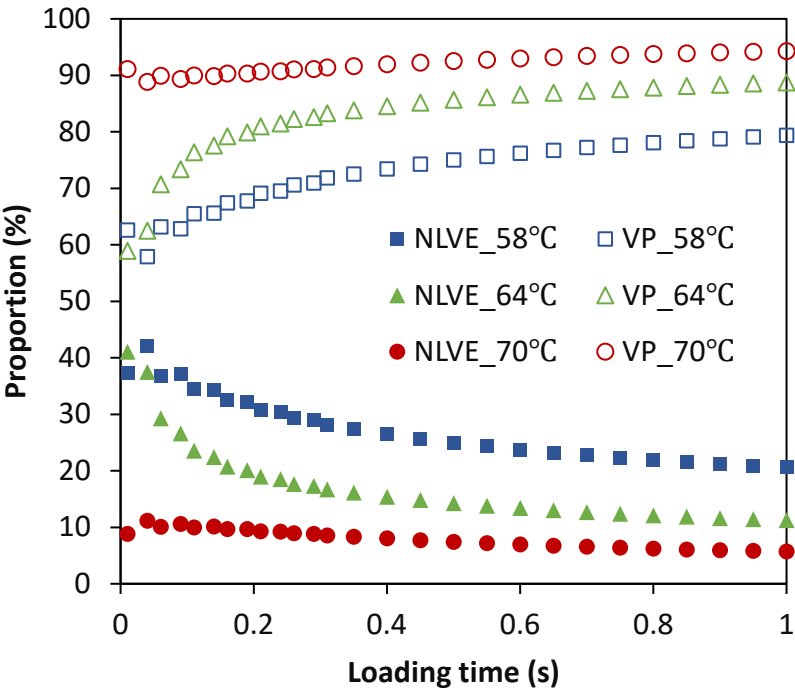


(c)

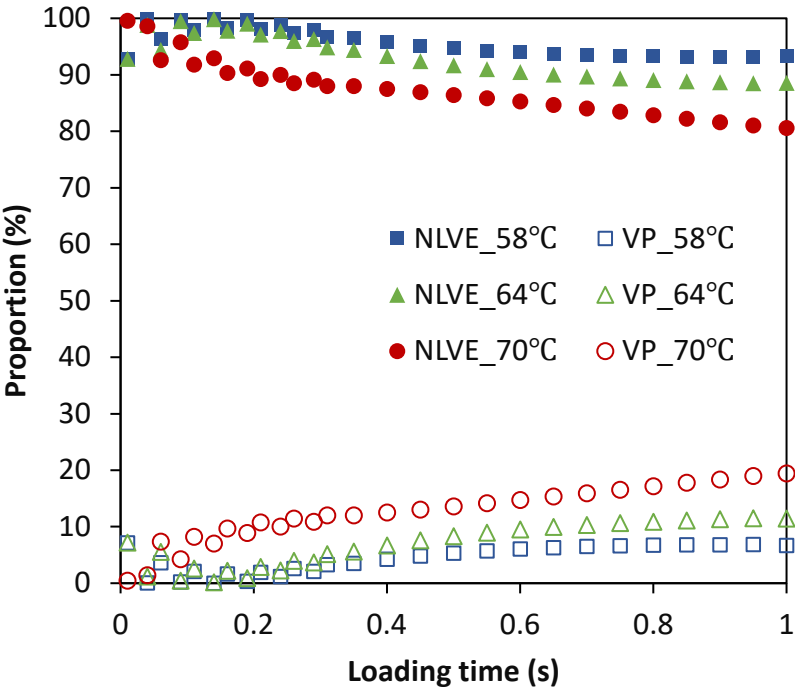
**Figure 5.** Nonlinear viscoelastic, viscoplastic strain and total strain in creep and recovery phase of three types of asphalt binders (VB, HVB and RB) at 58°C: (a) VB; (b) HVB; (c) RB

Figure 6 plots the proportions of the nonlinear viscoelastic strain, the viscoplastic strain of three types of asphalt binders (VB, HVB and RB) at three temperatures (58°C, 64°C and 70°C). In the legend, “NLVE” stands for the nonlinear viscoelasticity and “VP” stands for the viscoplasticity of the asphalt binders. It can be observed from Figure 6 that the proportion of the viscoplastic strain is larger than the nonlinear viscoelastic strain for VB (the proportion exceeds 60%), while it’s opposite for HVB and RB. This is because additives can improve the viscoplastic deformation resistance of the modified asphalt binders compared with the virgin asphalt binders without any additives. Besides, the proportion of the viscoplastic strain increases with the increase of the temperature for VB, HVB and RB, while the nonlinear viscoelastic strain is opposite. This is because the asphalt binders will gradually soften as the temperature increases, and more energy drives viscoplastic deformation of the asphalt binders compared with that at the lower temperature. In addition, the proportion of viscoplastic strain increases with the loading time for VB, HVB and RB at the three temperatures,

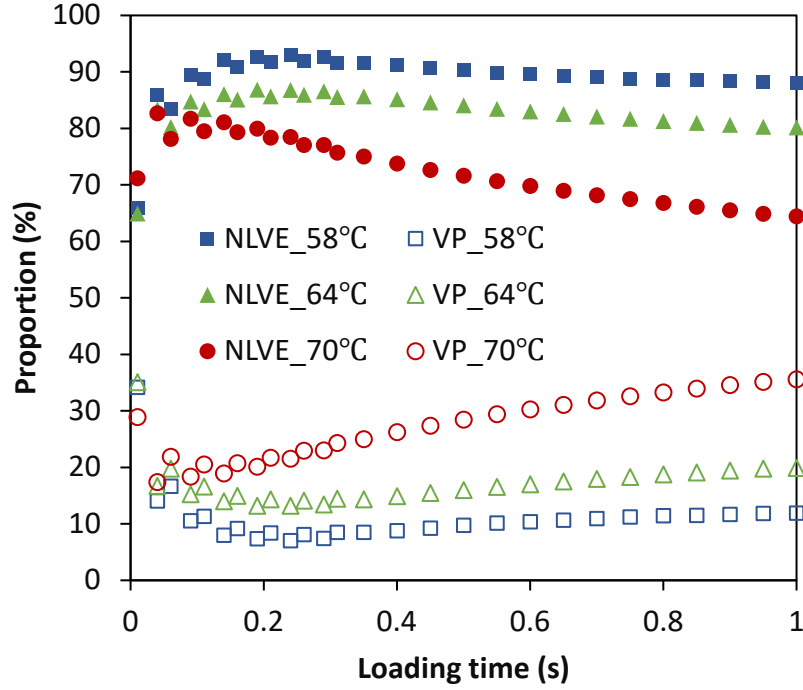
496 while the proportion of the nonlinear viscoelastic strain is opposite. It indicates that the viscoplastic  
497 strain is accumulated more quickly than the nonlinear viscoelastic strain of asphalt binders.



(a)



(b)



(c)

**Figure 6.** Proportions of the nonlinear viscoelastic strain, the viscoplastic strain of three types of asphalt binders (VB, HVB and RB) at three temperatures (58°C, 64°C and 70°C): (a) VB; (b) HVB; (c) RB

In addition, the non-recoverable creep compliance  $J_{nr}$  has been widely used to evaluate the viscoplastic deformation of asphalt binders (D'Angelo et al., 2009). In the standard calculation method,  $J_{nr}$  is calculated by the residual strain in the recovery phase and applied creep stress. However, the residual strain in the last loading time contains viscoplastic strain and not fully recovered nonlinear viscoelastic strain. Therefore, the standard calculation method for  $J_{nr}$  is inaccurate because the nonlinear viscoelastic strain is not fully recovered. In this study, the viscoplastic strain and nonlinear viscoelastic strain are separated. Hence, the viscoplastic strain can be determined for three types of asphalt binders accurately. To improve the calculation accuracy of the non-recoverable creep compliance,  $J_{nr}$  can be redefined as:

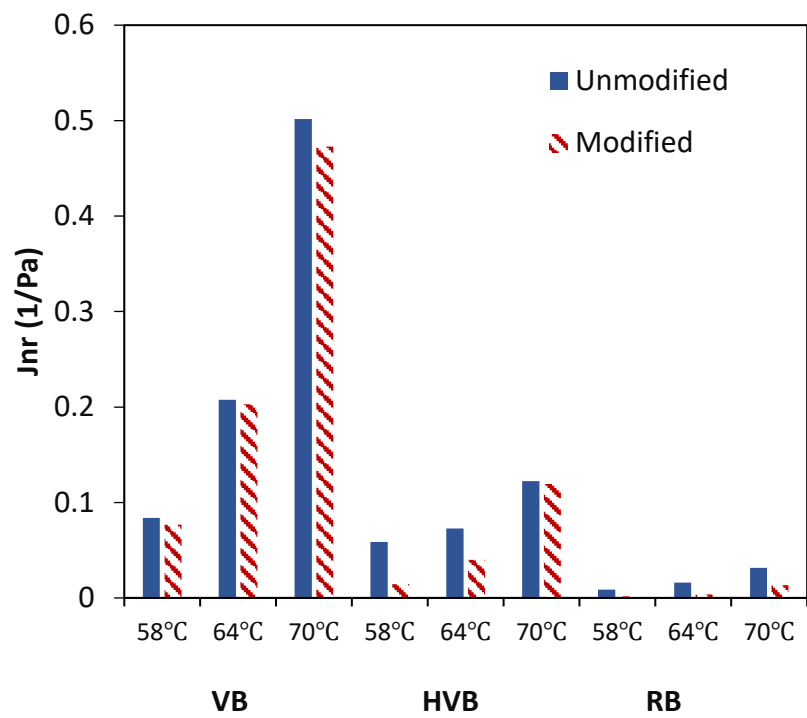
$$J_{nr}^m = \frac{\varepsilon_{vp}}{\sigma_p} \quad (38)$$

where  $J_{nr}^m$  is modified non-recoverable creep compliance of the asphalt binders in the creep and

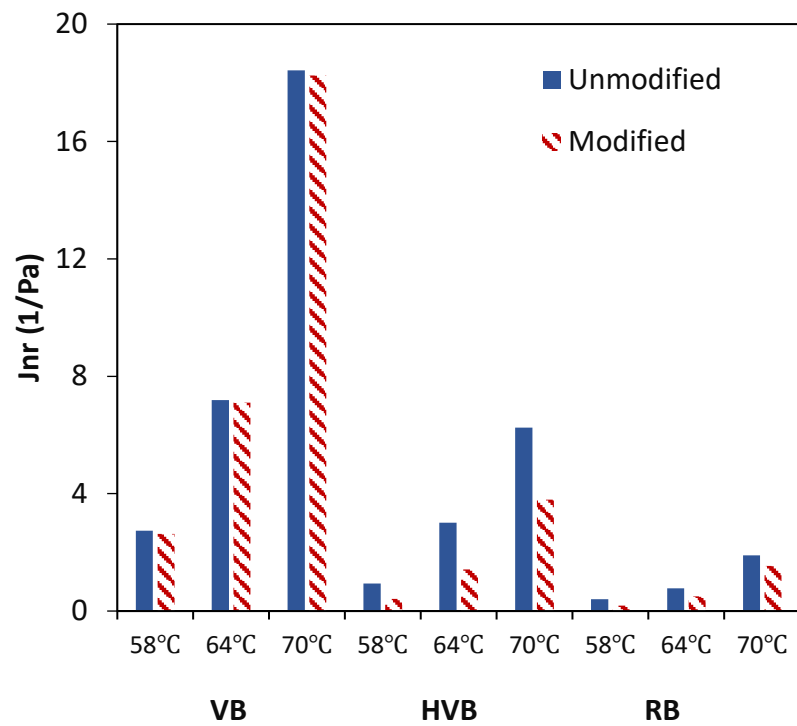
519 recovery test.

520 Figure 7 presents the comparison between unmodified  $J_{nr}$  and modified  $J_{nr}^m$  at three temperatures  
521 (58°C, 64°C and 70°C), two creep stress levels (0.1kPa and 3.2kPa), as well as their difference  
522 percentage. The following findings can be obtained: (1) the unmodified  $J_{nr}$  is larger than the  
523 modified  $J_{nr}^m$  indicator at any temperatures, creep stress (0.1kPa and 3.2kPa) for all binders; (2) the  
524  $J_{nr}^m$  indicator increases with the increase of the temperature, and creep stress level for all binders; (3)  
525 the  $J_{nr}^m$  indicator of VB is larger than those of HVB and RB, i.e., the order of viscoplasticity  
526 deformation resistance is RB>HVB>VB; and (4) different materials, temperatures and creep stress  
527 levels produce different difference percentages between unmodified  $J_{nr}$  and modified  $J_{nr}^m$ , the  
528 difference percentage of VB is minimum (less than 10%), while the difference percentages of HVB  
529 and RB are much larger (most are more than 50%).

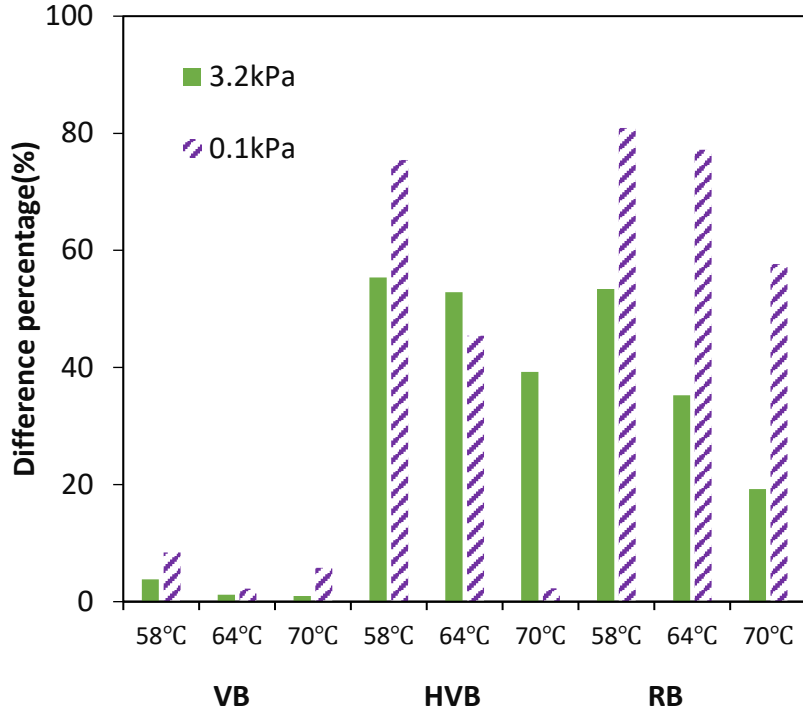
530 The reason for the finding (1) is that the modified  $J_{nr}^m$  is calculated by removing the total nonlinear  
531 viscoelastic strain, which is true “non-recoverable” creep compliance. The reason for finding (2) is  
532 that the viscoplastic strain increases with the increase of temperature and creep stress level. The  
533 reason for finding (3) is that the modified asphalt binders are strengthened by the interaction between  
534 the additives and virgin asphalt binders, leading to better viscoplastic deformation resistance of RB  
535 and HVB. The reason for finding (4) is that viscoplasticity is more dominant than nonlinear  
536 viscoelasticity for VB, while RB and HVB are opposite, which can be observed in Figure 6.



(a)



(b)



(c)

**Figure 7.** Comparison between unmodified and modified non-recoverable creep compliance at three temperatures (58°C, 64°C and 70°C), two creep stress levels (0.1kPa and 3.2kPa) and their difference percentage for three types of asphalt binders (VB, HVB and RB): (a) at 0.1kPa; (b) at 3.2kPa; (c) difference percentage of the unmodified and modified non-recoverable creep compliance

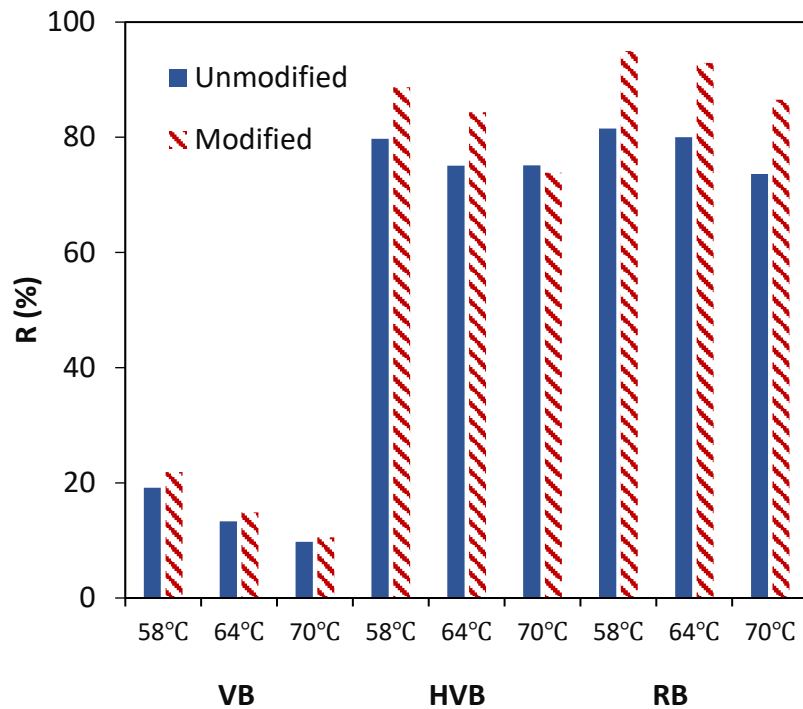
Furthermore, a percent recovery  $R$  is widely used to evaluate the recoverable ability of asphalt binders. However, the standard calculation approach of  $R$  is not accurate either, because the residual strain at the end of the recovery stage contains some parts of not fully recovered nonlinear viscoelastic strain. Similarly, to improve the calculation accuracy of the percent recovery, it can be redefined as:

$$R^m = \frac{\varepsilon^{NVVE}}{\varepsilon^{Total}} \times 100 = \frac{\varepsilon^{Total} - \varepsilon_{vp}}{\varepsilon^{Total}} \times 100 \quad (39)$$

where  $R^m$  is modified percent recovery;  $\varepsilon^{NVVE}$  is the recoverable nonlinear viscoelastic strain of the asphalt binders; and  $\varepsilon^{Total}$  is total creep strain, which is equal to the creep strain at the end of creep stage or the recovery strain at the initial recovery stage of the asphalt binders.

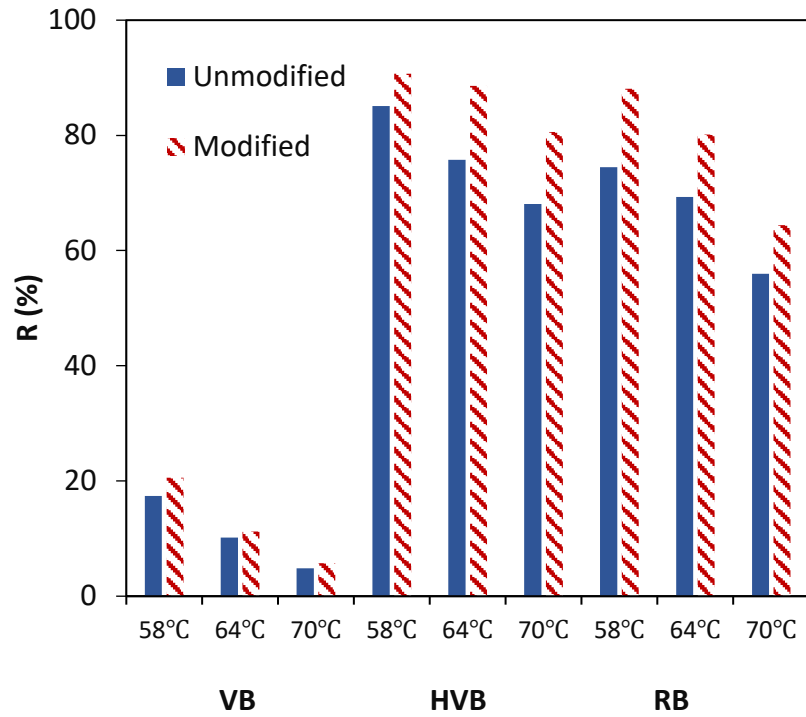
Figure 8 presents the comparison between unmodified percent recovery  $R$  and modified percent recovery  $R^m$  at different temperatures and creep stress levels, as well as their difference percentages for three types of asphalt binders. It can be found from Figure 8 that: (1) the unmodified percent recovery  $R$  is smaller than the modified  $R^m$  at any temperatures, creep stress (0.1kPa and 3.2kPa) for all binders, and most difference percentages between unmodified and modified percent recovery are more than 10% as shown in Figure 8c; (2) the  $R^m$  value of VB is the minimum; (3) the  $R^m$  values of all binders decrease with the increase of the temperature.

The reason for finding (1) is that the modified  $R^m$  is calculated by the “true” recoverable strain, while unmodified  $R$  is calculated by the residual strain at the end of the recovery stage. The reason for finding (2) is that VB without the additives is viscoplasticity dominant, while HVB and RB strengthened by the additives are dominated by nonlinear viscoelastic characteristics. The reason for the finding (3) is that all asphalt binders will produce viscoplastic deformation more easily at high temperatures.

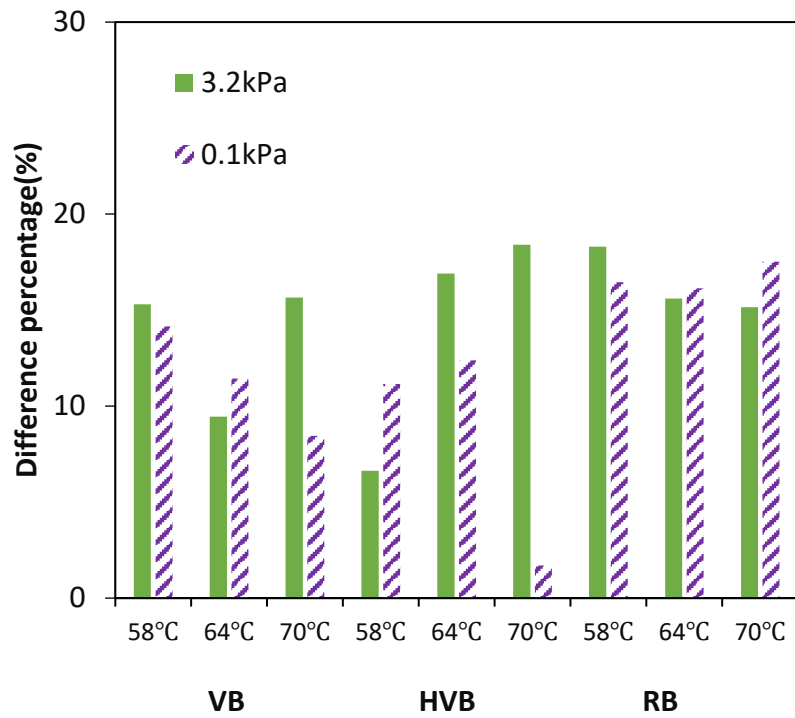


(a)





(b)



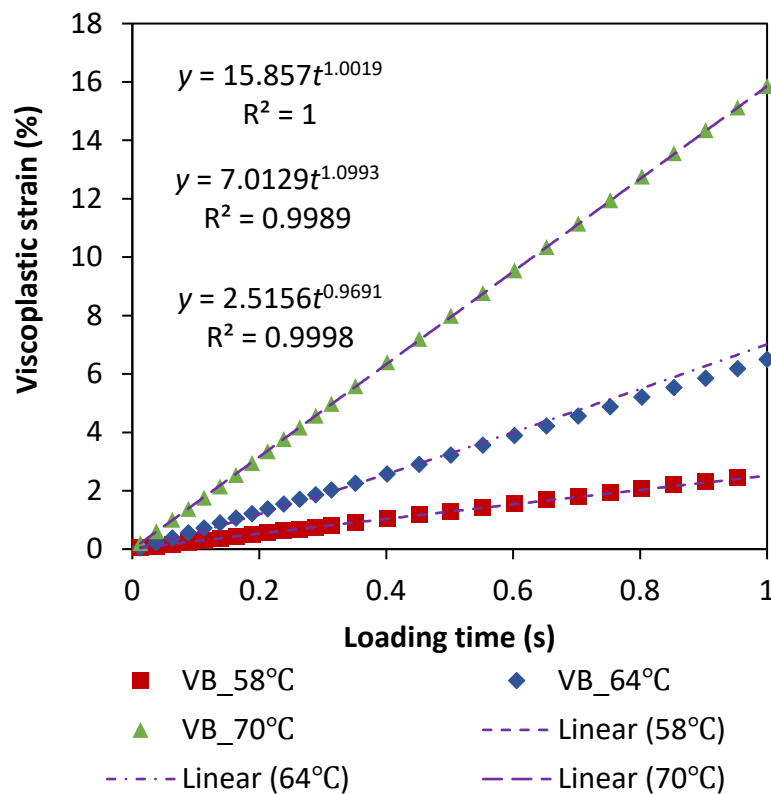
(c)

**Figure 8.** Comparison between unmodified and modified percent recovery at three temperatures (58°C, 64°C and 70°C), two creep stress levels (0.1kPa and 3.2kPa) and their difference percentage

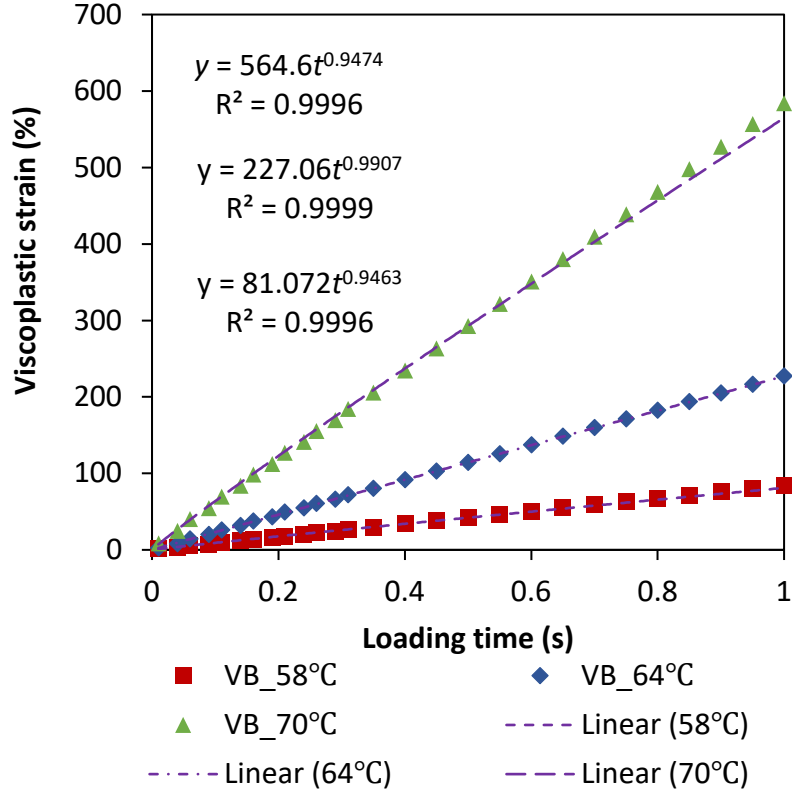
for three types of asphalt binders (VB, HVB and RB): (a) at 0.1kPa; (b) at 3.2kPa; (c) difference percentages of unmodified and modified percent recovery

### 4.3 Viscoplastic activation energy indicator

As can be seen from Figure 7 and Figure 8, the non-recoverable creep compliance and percent recovery are both affected by temperature and stress level. This study has also developed a temperature and stress-independent indicator (viscoplastic activation energy indicator) to characterize the viscoplasticity. Based on the separated viscoplastic strain, the viscoplastic strain rate can be obtained. Taking the VB as an example, Figure 9 shows the relationship between the viscoplastic strain and loading time of VB at two creep stress levels (0.1 and 3.2kPa) levels and three temperatures (58°C, 64°C and 70°C). The exponential term of the power function is almost equal to one, which indicates that the viscoplastic strain rate basically keep unchanged on this condition. The separated viscoplastic strain and viscoplastic strain model can match well at the two creep stress levels and three temperatures (the  $R^2$  values are larger than 0.9).



(a)



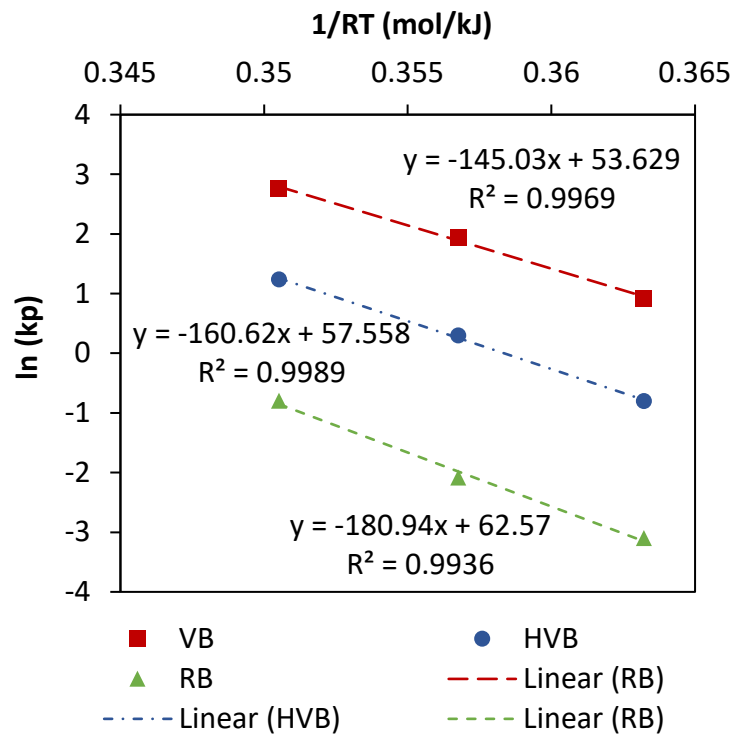
(b)

**Figure 9.** Relationship between the viscoplastic strain of VB and loading time at two creep stress levels (0.1 and 3.2kPa), three temperatures (58°C, 64°C and 70°C): (a) at 0.1kPa; (b) at 3.2kPa

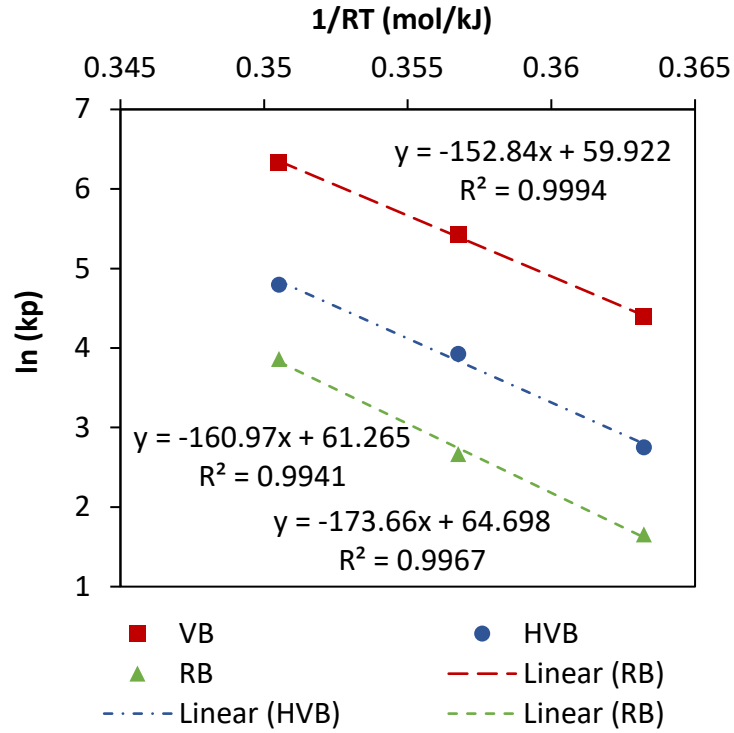
According to Eq. (29), the logarithm of the viscoplastic strain rate is linear with  $1/RT$  based on the analysis of the kinetics theory. This rule can be verified by the separated viscoplastic stain at the three temperatures. Figure 10 shows the relationship between the logarithm of the viscoplastic strain rate and  $1/RT$  of VB, HVB and RB at two creep stress levels (0.1 and 3.2kPa).  $\ln k_{vp}$  increases with the decrease of  $1/RT$ , because high temperature leads to faster viscoplastic deformation of the asphalt binders. Besides, the relationships between  $\ln k_{vp}$  and  $1/RT$  of VB, HVB and RB are linear (the  $R^2$  values are larger than 0.99). Hence, Eq. (29) is verified, i.e., the viscoplastic deformation process can be well modeled by the kinetic theory. In this way, the viscoplasticity of asphalt binders at different temperatures is correlated and the viscoplastic strain rate of asphalt binders at different temperatures can be predicted based on the viscoplastic strain kinetics model (Eq. (29)).

Figure 11 presents the viscoplastic activation energy of three types of asphalt binders at two creep

610 stress levels. It can be seen that the order of the viscoplastic activation energy of the binders is  
 611  $VB < HVB < RB$ . According to the kinetics theory, the greater the viscoplastic activation energy, the  
 612 greater the energy required for viscoplastic deformation. Hence, the order of viscoplastic  
 613 deformation resistance is  $VB < HVB < RB$ . Furthermore, the viscoplastic activation energy at the two  
 614 stress levels (0.1kPa and 3.2kPa) are basically the same, which indicates that the viscoplastic  
 615 activation energy is independent of the loading level (0.1kPa and 3.2kPa), which is consistent with  
 616 the findings on the cracking activation energy of asphalt binders (Li et al., 2021). Therefore, the  
 617 viscoplastic activation energy can be used as a characteristic indicator only related to the viscoplastic  
 618 deformation process of the nonlinear viscoelastic viscoplastic materials, which can be used to  
 619 evaluate the viscoplastic deformation resistance for the nonlinear viscoelastic viscoplastic materials.



(a)



(b)

**Figure 10.** Relationship between the logarithm of the viscoplastic strain rate and  $1/RT$  of three types of asphalt binders (VB, HVB and RB) at two creep stress levels (0.1 and 3.2kPa): (a) at 0.1kPa; (b) at 3.2kPa

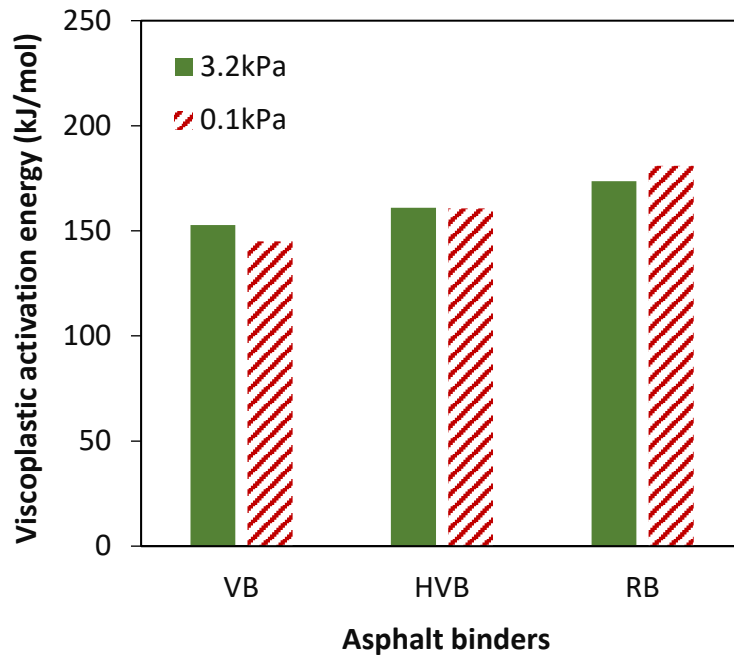


**Figure 11.** Viscoplastic activation energy of three types of asphalt binders (VB, HVB and RB) at two creep stress levels (0.1 and 3.2kPa)

## 5. Findings and future work

This study investigates the viscoplasticity coupled with the nonlinear viscoelasticity and proposes a new viscoplastic evaluation indicator that considers the influence of the temperatures and loading levels for the nonlinear viscoelastic viscoplastic materials. The following points summarize the main findings of this study:

- For any nonlinear viscoelastic material, nonlinear viscoelastic parameter  $g_1$  only affects the creep strain response, while nonlinear viscoelastic parameter  $g_2$  and  $a_\sigma$  both affect the creep and recovery strain response; and the effect of  $g_1$  and  $g_2$  on the strain response is more significant than  $a_\sigma$ . For asphalt binders,  $g_1$  is always equal to one and will not affect the nonlinear viscoelastic behavior of the asphalt binders.
- The proportion of the viscoplastic strain is larger than the nonlinear viscoelastic strain for VB (the proportion exceeds 60%), while it's opposite for HVB and RB; and the proportion of the viscoplastic strain increases with the increase of the temperature and loading time for VB, HVB and RB, while the nonlinear viscoelastic strain presents the opposite trend.
- The non-recoverable creep compliance and percent recovery are redefined based on the viscoplastic strain and nonlinear viscoelastic strain, which can accurately characterize the viscoplastic deformation and strain recovery ratio of asphalt binders comparing with the standard indicator.
- The logarithm of the viscoplastic strain rate has a linear relationship with the reciprocal of the temperature, and it increases with the decrease of the reciprocal of the temperature. The viscoplastic strain rates of asphalt binders at different temperatures are correlated, and their relationship can be predicted based on the established kinetics-based viscoplastic model.
- The viscoplastic activation energy indicator is proposed to characterize the viscoplastic deformation resistance for the nonlinear viscoelastic viscoplastic materials. The greater the viscoplastic activation energy, the greater the energy required for producing viscoplastic deformation. The order of viscoplastic deformation resistance of the asphalt binders is: VB<HVB<RB, based on the viscoplastic activation energy indicator.

657 In the future study, more materials and conditions will be employed to investigate the nonlinear  
658 viscoelasticity and viscoplasticity, which will provide more solid evidence to understand the  
659 mechanical behavior of the nonlinear viscoelastic viscoplastic materials.

660

## 661 **Acknowledgments**

662 This research was sponsored by National Key R&D Program of China under Grant No.  
663 2019YFE0117600, Project 52108423 supported by National Natural Science Foundation of China,  
664 and Zhejiang Provincial Natural Science Foundation of China under Grant No. LZ21E080002.

665

## 666 **References**

- 667 1. D'Angelo, J. A. (2009). The relationship of the MSCR test to rutting. *Road Materials and*  
668 *Pavement Design*, 10(sup1), 61-80.
- 669 2. Tabatabaee, N., & Tabatabaee, H. A. (2010). Multiple stress creep and recovery and time sweep  
670 fatigue tests: Crumb rubber modified binder and mixture performance. *Transportation Research*  
671 *Record*, 2180(1), 67-74.
- 672 3. Laukkanen, O. V., Soenen, H., Pellinen, T., Heyrman, S., & Lemoine, G. (2015). Creep-recovery  
673 behavior of bituminous binders and its relation to asphalt mixture rutting. *Materials and*  
674 *Structures*, 48(12), 4039-4053.
- 675 4. Walubita, L. F., Ling, M., Pianeta, L. M. R., Fuentes, L., Komba, J. J., & Mabrouk, G. M. (2022).  
676 Correlating the asphalt-binder MSCR test results to the HMA HWTT and field rutting  
677 performance. *Journal of Transportation Engineering, Part B: Pavements*, 148(3), 04022047.
- 678 5. Singh, B., & Kumar, P. (2022). Rutting and fatigue performance of aged modified asphalt  
679 binders. *International Journal of Pavement Research and Technology*, 15(4), 789-802.
- 680 6. Kennedy, T. W., Huber, G. A., Harrigan, E. T., Cominsky, R. J., Hughes, C. S., Von Quintus, H.,  
681 & Moulthrop, J. S. (1994). Superior performing asphalt pavements (Superpave): The product of  
682 the SHRP asphalt research program.
- 683 7. Sybilski, D. (1996). Zero-shear viscosity of bituminous binder and its relation to bituminous

mixture's rutting resistance. *Transportation Research Record*, 1535(1), 15-21.

8. Morea, F., Agnusdei, J. O., & Zerbino, R. (2011). The use of asphalt low shear viscosity to predict permanent deformation performance of asphalt concrete. *Materials and structures*, 44(7), 1241-1248.
9. Bahia, H. U., Hanson, D. I., Zeng, M., Zhai, H., Khatri, M. A., & Anderson, R. M. (2001). *Characterization of modified asphalt binders in superpave mix design* (No. Project 9-10 FY'96).
10. Lu, W., Peng, X., Lv, S., Yang, Y., Wang, J., Wang, Z., & Xie, N. (2023). High-temperature properties and aging resistance of rock asphalt ash modified asphalt based on rutting index. *Construction and Building Materials*, 363, 129774.
11. Shirzad, S., Idris, I. I., Hassan, M., & Mohammad, L. N. (2023). Self-Healing Capability and Mechanical Properties of Asphalt Mixtures Prepared With Light-Activated Polyurethane Prepolymer Modified Asphalt Binder. *Transportation Research Record*, 03611981221138522.
12. Padhan, R. K., Leng, Z., Sreeram, A., & Xu, X. (2020). Compound modification of asphalt with styrene-butadiene-styrene and waste polyethylene terephthalate functionalized additives. *Journal of Cleaner Production*, 277, 124286.
13. Leng, Z., Padhan, R. K., & Sreeram, A. (2018a). Production of a sustainable paving material through chemical recycling of waste PET into crumb rubber modified asphalt. *Journal of cleaner production*, 180, 682-688.
14. Leng, Z., Sreeram, A., Padhan, R. K., & Tan, Z. (2018b). Value-added application of waste PET based additives in bituminous mixtures containing high percentage of reclaimed asphalt pavement (RAP). *Journal of cleaner production*, 196, 615-625.
15. Tsantilis, L., Underwood, S. B., Miglietta, F., Riviera, P. P., Baglieri, O., & Santagata, E. (2021). Ageing effects on the linear and nonlinear viscoelasticity of bituminous binders. *Road Materials and Pavement Design*, 22(sup1), S37-S50.
16. Delgadillo, R., Bahia, H. U., & Lakes, R. (2012). A nonlinear constitutive relationship for asphalt binders. *Materials and structures*, 45(3), 457-473.
17. Masad, E. A., Huang, C. W., D'Angelo, J., & Little, D. N. (2009). Characterization of asphalt



binder resistance to permanent deformation based on nonlinear viscoelastic analysis of multiple stress creep recovery (MSCR) test. *Journal of the Association of Asphalt Paving Technologists*, 78.

18. Nivitha, M. R., Narayan, S. A., & Krishnan, J. M. (2018). Non-linear viscoelastic model based ranking of modified binders for their rutting performance. *Materials and Structures*, 51(4), 1-14.
19. Sun, Y., Chen, J., Huang, B., Liu, J., Wang, W., & Xu, B. (2020). Novel procedure for accurately characterizing nonlinear viscoelastic and irrecoverable behaviors of asphalt binders. *International Journal of Geomechanics*, 20(3), 04019198.
20. D'Angelo, J., & Dongré, R. (2009). Practical use of multiple stress creep and recovery test: Characterization of styrene-butadiene-styrene dispersion and other additives in polymer-modified asphalt binders. *Transportation Research Record*, 2126(1), 73-82.
21. AASHTO (2014) Standard method of test for multiple stress creep recovery (MSCR) test of asphalt binder using a dynamic shear rheometer (DSR). *AASHTO T 350-14*, Washington, DC.
22. Schapery, R. A. (1966). *A theory of non-linear thermoviscoelasticity based on irreversible thermodynamics* (pp. 511-530). New York, NY: American Society of Mechanical Engineers.
23. Schapery, R. A. (1969). On the characterization of nonlinear viscoelastic materials. *Polymer Engineering & Science*, 9(4), 295-310.
24. Sadeq, M., Masad, E., Al-Khalid, H., Sirin, O., & Mehrez, L. (2018). Linear and nonlinear viscoelastic and viscoplastic analysis of asphalt binders with warm mix asphalt additives. *International Journal of Pavement Engineering*, 19(10), 857-864.
25. Liu, H., Zeiada, W., Al-Khateeb, G. G., Ezzet, H., Shanableh, A., & Samarai, M. (2021). Analysis of MSCR test results for asphalt binders with improved accuracy. *Materials and Structures*, 54(2), 1-14.
26. Shirodkar, P., Mehta, Y., Nolan, A., Dahm, K., Dusseau, R., & McCarthy, L. (2012). Characterization of creep and recovery curve of polymer modified binder. *Construction and Building Materials*, 34, 504-511.
27. Brinson, H. F., & Brinson, L. C. (2008). Polymer engineering science and viscoelasticity. *An introduction*.

- 740 28. Luo, X., Li, H., Deng, Y., & Zhang, Y. (2020). Energy-Based kinetics approach for coupled  
741 viscoplasticity and viscofracture of asphalt mixtures. *Journal of Engineering Mechanics*, 146(9),  
742 04020100.
- 743 29. Zhang, Y., Birgisson, B., & Lytton, R. L. (2016). Weak form equation-based finite-element  
744 modeling of viscoelastic asphalt mixtures. *Journal of Materials in Civil Engineering*, 28(2),  
745 04015115.
- 746 30. Perzyna, P. (1966). Fundamental problems in viscoplasticity. *Advances in applied mechanics*, 9,  
747 243-377.
- 748 31. Bamford, C. H. and Tipper, C. F. H. eds. (1969). *Comprehensive Chemical Kinetics: The theory*  
749 *of kinetics* (Vol. 2). Elsevier Scientific Publishing Company, Amsterdam, The Netherlands.
- 750 32. Luo, X., Birgisson, B., & Lytton, R. L. (2020). Kinetics of healing of asphalt mixtures. *Journal*  
751 *of Cleaner Production*, 252, 119790.
- 752 33. Li, H., Luo, X., & Zhang, Y. (2021). A kinetics-based model of fatigue crack growth rate in  
753 bituminous material. *International Journal of Fatigue*, 148, 106185.
- 754 34. Luo, X., Gu, F., & Lytton, R. L. (2015). Prediction of field aging gradient in asphalt  
755 pavements. *Transportation Research Record*, 2507(1), 19-28.
- 756 35. Luo, X., Gu, F., & Lytton, R. L. (2019). Kinetics-based aging prediction of asphalt mixtures  
757 using field deflection data. *International Journal of Pavement Engineering*, 20(3), 287-297.
- 758 36. Luo, X., Gu, F., Zhang, Y., Lytton, R. L., & Birgisson, B. (2018). Kinetics-based aging  
759 evaluation of in-service recycled asphalt pavement. *Journal of Cleaner Production*, 200,  
760 934-944.